

**August 2013**

**Ph.D. Dissertation**

**Molecular Modeling Study of  
Human Chemokine CCR2 Receptor**

**Graduate School of Chosun University**

**Department of Bio-New Drug Development**

**Kothandan Gagan**

# **Molecular Modeling Study of Human Chemokine CCR2 Receptor**

인간 케모카인 CCR2 억제제의 분자모델링 연구

23<sup>rd</sup> August 2013

**Graduate School of Chosun University**

**Department of Bio-New Drug Development**

**Kothandan Gagan**

# **Molecular Modeling Study of Human Chemokine CCR2 Receptor**

**Advisor: Prof. Seung Joo Cho**

*This dissertation is submitted to the Graduate School of  
Chosun University in partial fulfillment of the requirements  
for the degree of Doctor of Philosophy in Science*

**June 2013**

**Graduate School of Chosun University**

**Department of Bio-New Drug Development**

**Kothandan Gugan**

**This is to certify that the Ph.D. dissertation of  
Kothandan Gugan has successfully met the  
dissertation requirements of Chosun  
University.**

**Chairman: Chosun Univ, Prof. Song Yub Shin** .....

**Member: Chosun Univ, Prof. Eun Ae Kim** .....

**Member: Chosun Univ, Prof. Ryu Seol** .....

**Member: Chonnam Univ, Prof. Chang Hyun Dam** .....

**Member: Chosun Univ, Prof. Seung Joo Cho** .....

**June 2013**

**Graduate School of Chosun University**

# Contents

<b>List of Tables</b> .....	<b>iii</b>
<b>List of Figures</b> .....	<b>iv</b>
<b>Abstract</b> .....	<b>viii</b>
<b>1. Introduction</b> .....	<b>1</b>
<b>2. Materials and Methods</b> .....	<b>5</b>
2.1 Sequence analysis of CCR2 .....	5
2.2 Homology modeling of CCR2 .....	5
2.3 Dataset used in this study .....	6
2.4 Binding site construction and docking analysis .....	17
2.5 Setup of the system in bilayer environment .....	18
<b>3. Results</b> .....	<b>20</b>
3.1 Sequence analysis of CCR2 .....	20
3.2. Homology modeling of CCR2 .....	23
3.3. Prediction of interaction between potent 4AAC antagonist and CCR2 receptor .....	28
3.3.1 Binding site of CCR2 .....	28
3.3.2 Docking studies of highly active CCR2 antagonist (compound 16b of 4AAC) .....	31

3.4 Molecular dynamics simulation of Receptor-Ligand-Membrane complexes .....	36
3.4.1 Setting up of CCR2-16b of 4AAC-lipid for the production run .....	37
3.4.2 Structural analysis of CCR2-4AAC complexes throughout production runs .....	39
3.4.3 Binding mode (CCR2-16b of 4AAC) and trajectory analysis .....	43
3.4.4 SAR studies of 4-azetidiny1-1-aryl-cyclohexane derivatives .....	53
3.4.5 Comparison of other potent antagonists with the MD simulated model .....	54
3.5 Comparative analysis of CCR2 and CCR5 .....	57
<b>4. Discussion</b> .....	<b>60</b>
<b>5. Conclusion</b> .....	<b>64</b>
<b>References</b> .....	<b>65</b>
<b>Appendix</b> .....	<b>79</b>

## List of Tables

Table 1. Structure and biological values of 4-Azetidinyl-1-aryl-cyclohexane derivatives .....	7
Table 2. Structure and biological values of 4-Azetidinyl-1-aryl-cyclohexane derivatives .....	13
Table 3. Representative set of CCR2 antagonists to derive the binding mode from the perspectives of binding site .....	56

## List of Figures

Figure 1 Alignment obtained between the query (CCR2) and template (PDB code: 3ODU) sequences for modeling. Identical residues are marked (\*), similar regions are marked (:). Secondary structure (TM domains) of the CCR2 receptor is indicated below the sequence in a cylindrical shape.

..... 22

Figure 2 Homology model (green) of CCR2 obtained and its refinement by MDS superimposed on the template structure CXCR4 (red). ..... 25

Figure 3a Ramachandran plot of the developed CCR2 model refined by MDS. Different color codes indicate most favored (red), generously allowed (dark yellow), additionally allowed (light yellow), and disallowed (white) regions ..... 26

Figure 3b: ProsA energy plot for the developed CCR2 model refined by MD simulation. .... 27

Figure 4a: Front view of the proposed binding pocket (CCR2). Binding site residues are colored based on atom types. Figure generated using the Pymol program (<http://www.pymol.org>). ..... 29

Figure 4b: Top view of the CCR2 binding pocket. Transmembrane (TM) helices are colored green, whereas the constructed binding pocket residues were color-coded with different colors depending on atom types. All TM



regions are labeled in red on the tops of helices. Figure generated using the Pymol program (<http://www.pymol.org>). ..... 30

Figure 5a: : Docked mode of compound 16b inside the proposed binding pocket of CCR2. Front view of the docked conformation of 16b. Binding site residues (carbon cyan, nitrogen blue and oxygen red) and the ligand molecule (carbon yellow, nitrogen blue and oxygen red) are colored based on atom types. Figure generated using the Pymol program (<http://www.pymol.org>). ..... 34

Figure 5b: : Alternative binding mode of compound 16b inside the proposed binding pocket of CCR2. Front view of the docked conformation of 16b. Binding site residues (carbon cyan, nitrogen blue and oxygen red) and the ligand molecule (carbon yellow, nitrogen blue and oxygen red) are colored based on atom types. Figure generated using the Pymol program (<http://www.pymol.org>). ..... 35

Figure 6: Side view of CCR2-ligand-membrane-aqueous environment for a production runs of 20 ns MDS. Seven transmembrane helices are represented as cartoons, the ligand molecule as a surface, lipid molecules as lines, and water molecules as sticks. Figure generated using the Pymol program (<http://www.pymol.org>). ..... 38

Figure 7: (a) Total energy plot of the MD simulation and variations in system total energy over 20 ns. (b) Root mean square deviation (RMSD) plot for CCR2 C from initial structures throughout the 20 ns simulation as a function of time. (c) Root mean square deviation (RMSD) plot for DRG as ligand throughout the 20 ns simulation. .... 41

Figure 8: (a) Root mean square deviation (RMSD) plot for CCR2 C from initial structures throughout the 20 ns simulation as a function of time. (b) Root mean square deviation (RMSD) plot for DRG as ligand throughout the 20 ns simulation. .... 42

Figure 9: Front view of the docked mode of compound 16b inside the proposed binding pocket of CCR2 after MDS. Binding site residues (carbon cyan, nitrogen blue and oxygen red) and the ligand molecule (carbon yellow, nitrogen blue and oxygen red) are colored according to atom type. .... 44

Figure 10: Minimum distances between the 16b and CCR2 active site residues surrounding 4 Å were computed using MD simulation trajectories. (a) Tyr49 and 16b, (b) Trp98 and 16b and (c) Ser101 and 16b. Minimum distances were calculated and plotted as a function of time. .... 46

Figure 11: Minimum distances between Glu291 (Oxygen atom) and 16b (basic nitrogen in azetidiny ring) computed using MD simulation

trajectories. Minimum distances were calculated and plotted as a function of time. ....	48
Figure 12: Minimum distances between (a) Tyr120 and 16b and (b) His121 and 16b. Minimum distances were calculated and plotted as a function of time. ....	49
Figure 13: Minimum distances between (a) Thr203 and 16b, (b) Arg206 and 16b and (c) Asn207 and 16b. Minimum distances were calculated and plotted as a function of time. ....	51
Figure 14: Minimum distances between (a) Tyr259 and 16b and (b) Ile263 and 16b. Minimum distances were calculated and plotted as a function of time. ....	52
Figure 15. Alignment obtained between the CCR2 and CCR5 sequences for sequence analysis. Identical residues are marked as (*), similar regions are marked as (:). ....	58
Figure 16. Superposition of varying residues in the active sites of CCR2 (cyan) and CCR5 (magenta). All the TM's are labeled by blue color on the top of helices. ....	59

## **Abstract**

# **Molecular Modeling Study of Human Chemokine CCR2 Receptor**

Kothandan Gugan

Advisor: Prof. Seung Joo Cho, Ph.D.

Department of Bio-New Drug Development

Graduate School of Chosun University

Chemokine receptor (CCR2) is a G protein-coupled receptor that contains seven transmembrane domains. Recent research has focused on the antagonism of CCR2 and several molecules are under various phases for varied disease conditions such as arthritis, multiple sclerosis, and type 2 diabetes. On account of its importance, CCR2 is an important target and information about this receptor is of prime importance. In this study, we analyzed the time dependent behavior of CCR2 complexed with potent CCR2 using MDS for a period of 20 ns by using in silico methodologies. Homology model of CCR2 was done and docking of a potent 4-azetidiny-1-aryl-cyclohexane derivative was docked into the binding site. The docked model was then inserted into a membrane model to study the dynamic behavior of enzyme complex and crucial insights were found. SAR relationships of 4-azetidiny-1-aryl-cyclohexane derivatives were performed and we also identified the reasons for activity and probable binding mode for some CCR2 antagonists from the perspectives of binding site. Our initial

model found that Tyr49, Ser101, Glu291 and some other residues are crucial. However, our MDS analysis found that Ser101 may not be vital, as the hydrogen bonding got vanished and the ligand moved away from it. Moreover we also found that Arg206, Asn207, Tyr259 might be crucial and mutagenesis studies on these residues could be effective. Comparative analysis of CCR2 and CCR5 binding site was done to facilitate the development of dual antagonists and also to address the issue of selectivity. Our results could be helpful to design potent and novel CCR2 antagonists and could be also be a starting point for structure based drug design.

Keywords: CCR2, Homology modeling, Molecular dynamic simulation, Molecular docking.

# 초 록

## 인간 케모카인 CCR2 억제제의 분자모델링 연구

코탄단 구간

지도교수: 조 승 주

바이오신약개발학과

케모카인 수용체인 CCR2는 일종의 G 단백질과 결합된 7개의 막을 관통하는 도메인을 포함한다. 최근의 연구는 CCR2의 억제에 초점을 맞추어 왔으며, 몇개의 분자가 관절염, 다발성 경화증, 2형 당뇨병등의 다양한 증상에 많은 임상연구가 진행중이다. CCR2는 중요한 작용점이고, 이 수용체에 관한 정보는 대단히 중요하다. 본 연구에서는, *in silico* 방법들을 이용하여, 20 ns 동안 분자동력학적인 방법으로 CCR2와 결합한 다양한 억제제들의 시간에 의존하는 행동을 분석하였다. CCR2의 호몰로지 모델을 만들었고, 강력한 4-azetidyl-1-aryl-cyclohexane 유도체들이 결합사이트로 결합되었다. 이 결합된 모델은 순차적으로 막모델속에 집어넣은 다음, 단백질과 리간드의 결합체의 동력학적인 행동을 연구한 결과 중요한 정보를 얻을 수 있었다. 특히, 구조 활성 상관관계에 대한 정보가 얻어졌다. CCR2 억제제의 결합모형과 관련하여 활성에 대한 물리적인 정보를 이해할 수 있었다. 초기의 결합 모형으로는

Tyr49, Ser101, Glu291를 비롯한 몇개의 아미노산 잔기가 중요했다. 그러나, 이 분자동역학 분석으로서 Ser101은 이것이 리간드로부터 멀어지는 것으로 보아서, 중요하지 않은 것으로 예측되었다. 더구나, Arg206, Asn207, Tyr259등이 대단히 중요한 잔기로서 돌연변이 연구에 중요할 것으로 판단되었다. CCR2와 CCR5의 결합부위의 비교연구로 부터, 양쪽 수용체에 작용할 수 있는 억제제를 개발하는 것도 가능해 보인다. 이 결과는 새로운 CCR2의 억제제를 설계하는데 도움이 되며, 또한 구조기반의 신약설계에 출발점이 될 것이다.

키워드 : CCR2, 상동 모델링, 분자 동적 시뮬레이션, 분자 도킹.

## **1. Introduction**

The chemokine receptor family includes ~20 G-protein-coupled receptors with the purpose of playing a central role in leukocyte migration and activation (1). Specific family members are also involved in viral entry and angiogenesis. With this diverse range of important functions, they have been targeted as potential points of pharmaceutical intervention for blunting diseases as diverse as asthma, rheumatoid arthritis, multiple sclerosis, solid organ transplantation and atherosclerosis, cancer, and HIV infection (2). In all instances, the promise of chemokine receptor antagonism has been one of selective therapy targeted at a critical portion of the disease process.

Chemokines are small (8-10 kDa) water-soluble proteins consisting of 340-380 amino acid residues, which play key roles in immuno-modulation and host defense. They selectively recruit monocytes, neutrophils, and lymphocytes to sites of vascular injury and inflammation (3, 4 and 5). Different chemokines produce different leukocyte responses depending on the complementary nature of their chemokine receptors (6, 7). The basic feature of inflammation is the tissue recruitment of leukocytes, which is mediated mainly by chemokines (chemotactic cytokines) via their receptors. The chemokine super family can be categorized into four groups (CC, CXC, CX3C, and C), according to the number and spacing of conserved cysteines in the amino acid sequence (2, 8 and 10). Apart from their well-recognized role in leukocyte recruitment, some other chemokines and chemokine receptors play some crucial roles in other cellular



functions such as activation, proliferation, and differentiation (2, 8 and 10).. Specific family members are also involved in viral entry and angiogenesis (2).

In particular, CCR2 is a G protein-coupled receptor that binds multiple ligands (macrophage chemoattractant proteins), including CCL2 (MCP-1), CCL8 (MCP-2), CCL7 (MCP-3), and CCL13 (MCP-4). The relative contribution of each of these ligands to CCR2-mediated in vivo function remains to be elucidated (9, 10). Of these ligands, MCP-1 is studied most comprehensively, and CCR2 is considered to be the elite receptor for MCP-1 (9, 10). The indispensable role of CCR2/MCP-1 axis in the tissue recruitment of monocytes/macrophages has been established by studies in which CCR2 or MCP-1 has been genetically ablated (11,12,13 and 14) and studies in which CCR2 or MCP-1 is pharmacologically inhibited (15, 16).

KO mice of CCR2 or MCP-1 are apparently healthy but exhibit an impaired ability to recruit monocytes/macrophages to sites of inflammation (17,18,19 and 20) and to produce cytokines such as TNF- (21, 22). The impaired recruitment of monocytes in CCR2 KO mice treated with a CCR2 antagonist can be explained by reduced mass departure of inflammatory monocytes from bone marrow to blood (22) and reduced immigration of blood monocytes from blood to inflamed tissues (17,18,19 and 20). Notably, the CCR2/MCP-1 axis is not important for monocyte adhesion but for migration into the inflamed tissue, such as atherosclerotic arteries (23.) Consistent with its key role in monocyte trafficking, CCR2 has been shown to drive inflammation in a number of animal models of diseases such as RA, CD, and transplant rejection, as

well as cardiovascular diseases, including atherosclerosis and AIH. Recent pharmaceutical research has focused on the antagonism of CCR2 and several molecules including CCX915 (ChemoCentryx), INCB3284 (Incyte and Pfizer), MK0812 (Merck), MLN1202 (Millennium Pharmaceuticals), and MCP-1 antagonist (Telik) are under various phases for varied disease conditions such as arthritis, multiple sclerosis, and type 2 diabetes. Owing to its importance, CCR2 is considered to be an attractive target in the field of drug discovery (24).

Computational modeling has become an essential tool in guiding and enabling rational decisions with respect to hypothesis driven biological research. Knowledge of the three dimensional structure of receptor (CCR2) is important for understanding the molecular mechanisms underlying the diseases caused by mutations. Though homology models are not the same as an experimentally determined structure of a given protein, it could provide a rational alternative and it is still very helpful in assisting researchers to understand the binding modes of lead molecules against its proposed target. The crystal structure of CCR2 has not yet been reported. In the absence of structural information, ligand-based approaches have proven to be especially useful for G protein-coupled receptor (GPCR) (25). However, a few studies based on modeled structures have also been reported (26, 27).

Numerous structural activity relationship studies of potent CCR2 antagonists have already been reported in the literature (28, 29). We also reported on quantitative structure activity relationship studies for CCR2 antagonists by developing 3D-QSAR

models using in silico methodologies (30) such as CoMFA and CoMSIA. However, there have been no attempts were reported to study the time dependent behavior of CCR2 with potent antagonists using molecular dynamic (MD) simulations and this prompted us to initiate the analysis.

In this study, we report on structure activity relationship studies of azetidiny-1-aryl-cyclohexanes as potent CCR2 antagonists using in silico methodology molecular dynamics simulations (CCR2-one of the highly active ligand). Our work deals with the application of various in silico methodologies such as comparative modeling, molecular docking and molecular dynamics simulation. A homology model of CCR2 was constructed by using CXCR4 (PDB code: 3ODU) as template (31) and the developed model was refined. Furthermore, a potent CCR2 antagonist (16b Of 4AAC) was docked inside the proposed binding site and in addition the final CCR2-ligand complex was subjected to a 20 ns MD simulation in the presence of DPPC/TIP3P membrane environment. The results helped in evaluating the stability of the binding site interactions as well as identify perturbations in the interaction profiles that would not be possible through docking studies. Based on the analysis and observations from this simulation studies, a number of critical suggestions could be made that would be helpful in future structure-based design efforts against this target. Comparative analysis of CCR2 and its close homology CCR5 was also done to facilitate the development of dual antagonist and to address the issue of selectivity.

## **2. Materials and Methods**

### **2.1 Sequence analysis of CCR2**

The entire amino acid sequence of human CCR2, which composed of 374 amino acids were retrieved from Uniprot database (accession number P41597). In order to identify an adequate template for modeling of CCR2 chemokine receptor, BLAST algorithm (32, 33) (Basic local alignment search tool for protein) search was carried out against the protein data bank (PDB) (34). The top template obtained with the aforementioned search against PDB was then selected to perform sequence alignment using ClustalW 2.0 (35) with default parameters.

### **2.2 Homology modeling of CCR2**

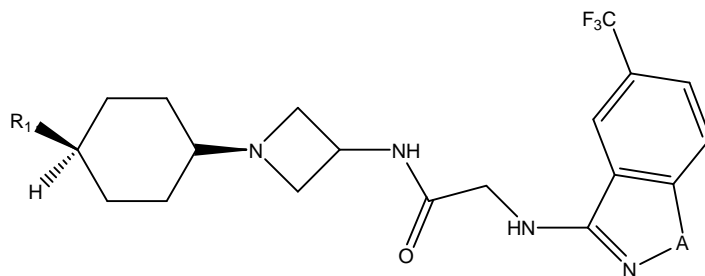
A number of homologous structures were identified as templates in the PDB. CXCR4 is reported as the top template. CXCR4 structure is a homodimer with A and B chains in it. As the template structure is homodimer, it is possible to use any of the chains. In this study we used A chain and sequence alignment was done with the A chain for modeling. With the sequence alignment obtained against top template structure, homology model of CCR2 was generated using Modeller9v4 program (36, 37 and 38). Modeller9v4 computes a model composed of non-hydrogen atoms based on aligning the sequence to be modeled with known related structures. A 3D model was obtained by optimization of a molecular probability density function (PDF) using a variable target function procedure in Cartesian space that employs methods of

conjugate gradients and molecular dynamics with simulated annealing. Fifty such 3D models were generated and for further computational study. Out of the generated models, model with a lower Molpdf (molecular probability density function) score and a lower root mean square deviation (RMSD) with that of the template (CXCR4) was selected. The best modeled structure was prepared using structure preparation tool under Biopolymer module within Sybyl v8.1 (39). This model was refined by performing energy minimization in a vacuum assumption to relax from the strain in the model. Steepest descent algorithm and Gromos53a6 force field was used for this refinement procedure. The selected model was further validated using PROCHECK [40], ERRAT [41], and ProSA (<https://prosa.services.came.sbg.ac.at/prosa.php>).

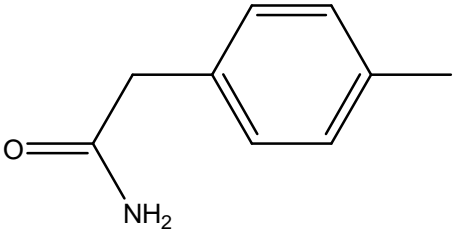
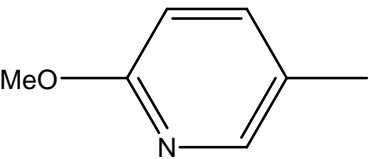
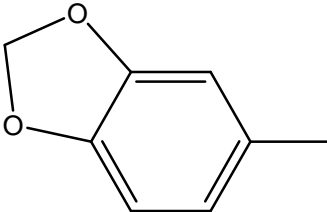
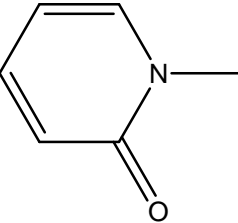
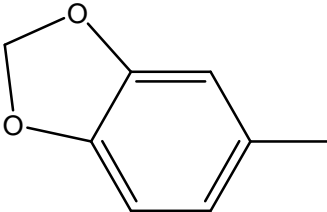
### **2.3. Dataset used in this study**

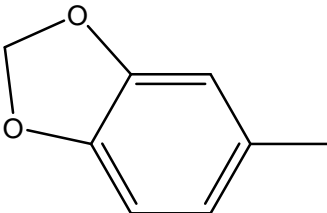
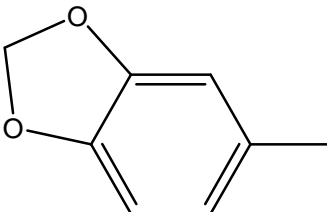
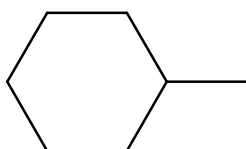
A series of potent CCR2 antagonists and their biological activities ( $IC_{50}$  values) have been previously reported by Zhang et al. (42). The geometries of ligand molecules were optimized using the Tripos force field methodology (43) using the distance-dependent dielectric and Powell's conjugate gradient method (44). Partial atomic charges were applied using Gasteiger Huckel charges (45). One of the most active compounds in the series reported by Zhang et al., compound 16b of 4AAC ( $IC_{50} = 5$  nM,  $pIC_{50} = 8.3$ ) was selected as the template molecule (**Table 1** and **Table 2**). The  $IC_{50}$  (nM) values of molecules used in this study were converted to corresponding  $pIC_{50} = (-\log IC_{50})$  values.

Table 1. Structure and biological values of 4-Azetidiny-1-aryl-cyclohexane derivatives



Compound	R1	A	IC <sub>50</sub> (nm)	pIC <sub>50</sub>
13a		NH	12	7.92
13b		NH	6	8.22

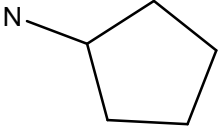
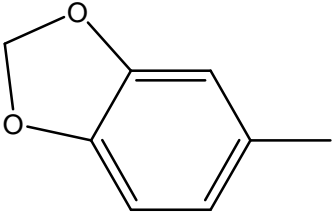
13c		NH	12	7.92
13d		NH	12	7.92
13e		NMe	13	7.88
13f		NH	63	7.20
13g		NCH <sub>2</sub> CH <sub>2</sub> OH	21	7.67

13h		NCONH-t-Bu	55	7.25
13i		NCONH <sub>2</sub>	82	7.08
14a	i-Pr	NH	370	6.43
14b	CN	NMe	330	6.48
14c		NMe	120	6.92
14d	CO <sub>2</sub> Et	NMe	13	7.88



14e	COOH	NMe	2600	5.58
14f	CONH <sub>2</sub>	NMe	510	6.29
14g	CH <sub>2</sub> OH	NMe	44	7.35
14h	CH <sub>2</sub> OEt	NMe	27	7.56
14i	CH <sub>2</sub> OCH <sub>2</sub> CH=CH <sub>2</sub>	NMe	32	7.49
14j	OH	NMe	530	6.27
14k	OEt	NMe	140	6.85
14l	OCH <sub>2</sub> CH=CH <sub>2</sub>	NMe	200	6.69

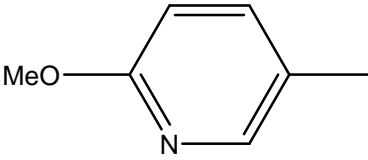
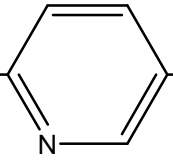
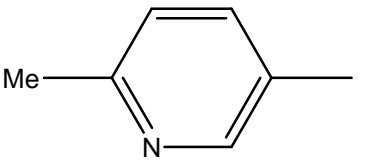
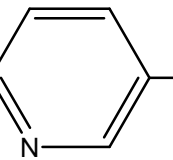
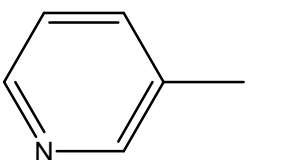
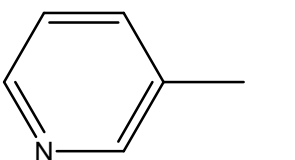
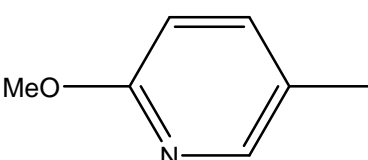
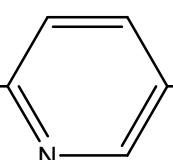
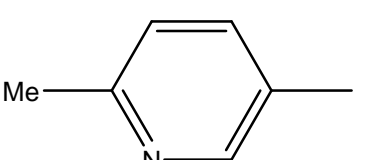
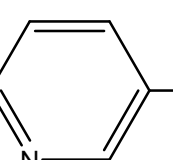
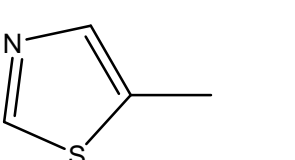
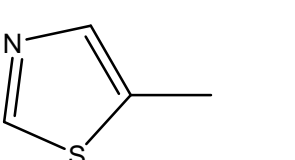
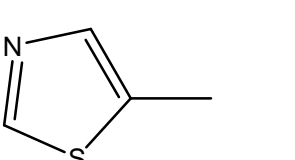
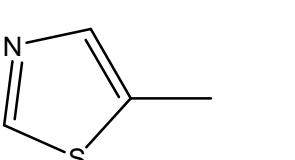
14m	NH <sub>2</sub>	NMe	>25000	-
14n	NHSO <sub>2</sub> Me	NMe	2080	5.68
14o	CO <sub>2</sub> Et	NH	27	7.56
14p	CO <sub>2</sub> Et	NEt	15	7.82
14q	CO <sub>2</sub> Et	NCH <sub>2</sub> CH=CH <sub>2</sub>	53	7.27
14r	CO <sub>2</sub> Et	NCH <sub>2</sub> CF <sub>3</sub>	230	6.63
14s	CO <sub>2</sub> Et	NCONH <sub>2</sub>	56	7.25

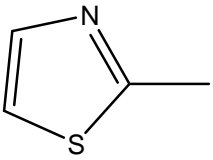
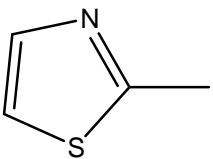
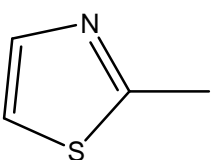
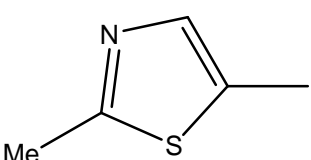
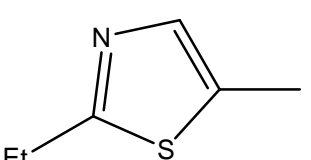
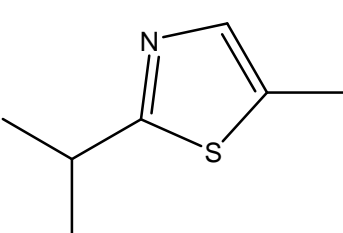
14t	CO <sub>2</sub> Et	NSO <sub>2</sub> Me	920	6.03
14u	CO <sub>2</sub> Et	Bn	170	6.76
14v	CO <sub>2</sub> Et		650	6.18
15a		O	36	7.44
15b	CO <sub>2</sub> Et	O	29	7.53

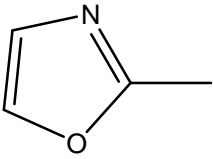
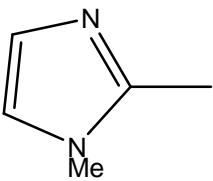
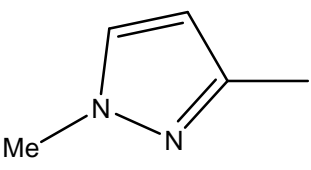
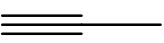
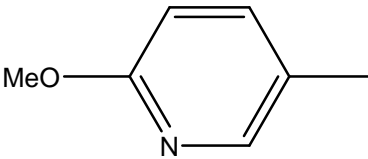
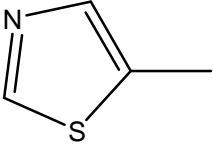
---

Table 2. Structure and biological values of 4-Azetidiny-1-aryl-cyclohexane derivatives

Compound	R1	A	IC <sub>50</sub> (nm)	pIC <sub>50</sub>
16a		NMe	19	7.21
16b		NMe	5	8.30
16c		NH	30	7.52

16d	 MeO- 	NH	16	7.79
16e	 Me- 	NH	6	8.22
16f	 	NMe	56	7.25
16g	 MeO- 	NMe	9	8.04
16h	 Me- 	NMe	7	8.15
16i	 	NH	16	7.79
16j	 	NMe	28	7.55

16k		NMe	13	7.88
16l		NCONH <sub>2</sub>	29	7.53
16m		CH <sub>2</sub> CH <sub>2</sub> OH	29	7.53
16n		NMe	19	7.72
16o		NMe	18	7.74
16p		NMe	5	8.30

16q		NMe	480	6.31
16r		NMe	1400	5.80
16s		NMe	200	6.69
16t		NMe	10000	5
15c		O	23	7.60
15d		O	31	7.50



## 2.4 Binding site construction and docking analysis

Autodock 4.0 program was used for the docking calculations. Autodock uses the Lamarckian genetic algorithm (LGA) and is regarded to be the best method in terms of the accuracies of its structural predictions and its ability to identify lowest energy structures (46). Hydrogen atoms and the active torsions of ligand were assigned using Autodock tools (ADT). The binding site for the receptor structure (CCR2) was assigned using previously published results. As we know that Glu291 is the crucial residue for ligand binding from previous reports, keeping this residue as starting point the binding site was extended (by 5 Å residues) up to 5 Å and modeled to guide the ligand molecule en route for possible orientation in the binding site. Autogrid was employed to generate grid maps around the active site using 60×60×60 points and a grid spacing of 0.375 Å. The docking parameters modified from defaults were; number of individuals in the population (set at 150), maximum number of energy evaluations (set at 2,500,000), maximum number of generations (set at 27,000), and number of GA runs (set at 50). The final structures were clustered and ranked according to the Autodock scoring function. Finally two conformers were selected according to the scoring



function, top cluster and using crucial residues determined by previous mutational studies and experimental studies.

## **2.5 Setup of the system in bilayer environment**

To study the time dependent behavior of CCR2-16b of 4AAC complexes, molecular dynamic simulation was done using GROMACS simulation package (47) in an explicit phospholipid bilayer. Protein, ligand, lipid and water molecules were used as components for the simulation. The GROMOS96 force field (47) was used and the lipid bilayer was developed using specific topology files, as described by Tieleman (48) (<http://moose.bio.ucalgary.ca>), was used in the present study.

To obtain a better starting structure, we used the InflateGRO script from Prof. Tieleman website (<http://moose.bio.ucalgary.ca>) (49) was used to pack lipids around an embedded protein. The starting point with this method is a pre-equilibrated bilayer into which the protein ligand complex has already been “inserted” in the lipid bilayer but fully overlaps with lipids. The system cannot be energy minimized due to extreme overlap. The bilayer was expanded using a scaling factor of 4 and a distance cut-off of 14 Å. Overlapping lipid molecules was deleted. For estimating the area per lipid a grid size of 5 Å was used. Energy minimization was done using strong position restraints to ensure that the structures (Protein-ligand) don't change at all. Energy minimization was then followed by compression using a scaling

factor of 0.95. Compression and energy minimization steps were repeated until the area per lipid converges to the reference value (0.62-0.64) for the lipid species used.

The system was then solvated with TIP3P water box (50) by increasing the van der Waals radius of carbon atoms from 0.15 to 0.5, so to prevent water molecules from being placed in the hydrophobic section of the bilayer (49). Once the system got solvated, the van der Waals radius of C was again set to 0.15 Å. The system was further neutralized by adding 27 Na<sup>+</sup> and 37 Cl<sup>-</sup> counter ions with a concentration of 0.15 M. Periodic boundary conditions were applied; the ligand topologies as well as the parameters were obtained from PRODRG server (51). The parameterization methodology implemented in the PRODRG program is widely used in MD simulations of drugs; however, the applicability of PRODRG charges for molecular simulations has been questioned in the literature, because PRODRG doesn't reproduce topologies in the force field due to inconsistent charges and charge groups (52). The partial charges are crucial in particular for a reasonably accurate description of non covalent interactions due to the long-range nature of electrostatic interactions and PRODRG underestimates charges for some atom types. To overcome this issue, we cross checked the topologies and we manually assigned charges with PM3 charges.

After energy minimization, the system was subjected to a short NVT equilibration phase and it is further followed by a longer NPT phase. Generally a short NVT equilibration phase is followed by a longer NPT phase. The

reason is that we are now dealing with a heterogeneous system [water and DPPC] as solvents. Such heterogeneity requires a longer equilibration process. Water has to reorient around the lipid head groups and any exposed parts of the protein, and the lipids have to orient themselves around the macromolecule. During equilibration, the macromolecule (protein-ligand) was position restrained so that it allows the solvents to equilibrate around our protein structure without any structural changes in the protein. NVT ensemble was done at constant temperature of 310 K for a period of 100 ps and then followed by NPT ensemble for a period of 1 ns. Modified Berendsen coupling scheme was employed in both the ensembles, particle mesh Ewald (PME) (53) method was used to calculate long-range electrostatics. Parinello and Rahman coupling scheme was used as barostat for pressure coupling and semi-isotropic pressure coupling was applied with reference pressure (1.0 bar), which is intended for membrane simulations. All bond lengths were constrained using the LINCS algorithm (54) and SETTLE algorithm was used to constrain the geometry of water molecules (55). Final production run was performed for a period of 20 ns.

### **3. Results**

#### **3.1. Sequence analysis of CCR2**

A BLAST search revealed that CXCR4 (PDB code: 3ODU) as the top template. The sequence identity between the template (3ODU) and the query sequence (CCR2) was 35%, and the identity between the active sites of the template and query

was 60%, which was encouraging. Whereas, the identity between the traditional bovine rhodopsin and CCR2 was found to be 21 % and the sequence identity with 2-adrenergic receptor was found to be 24%. Analysis showed high levels of homology between the target (CCR2) and template (CXCR4) sequences and better than that of traditional bovine rhodopsin and the more recent 2-adrenergic receptor templates. The reason for the high homology, overall and with the active site was that the template sequence was a close homologue (CXCR4). The more important step in the modeling procedure was to obtain acceptable alignment between target and template sequences. The alignment obtained using ClustalW 2.0 is shown in Figure 1. The E-value represents the number of different alignments with scores equivalent to or better than the scores expected to occur for a random database search. Generally, a lower E-value indicates that alignment is real not due to chance. The expectation value (E-value) for CCR2 was found to be  $2e-33$ .

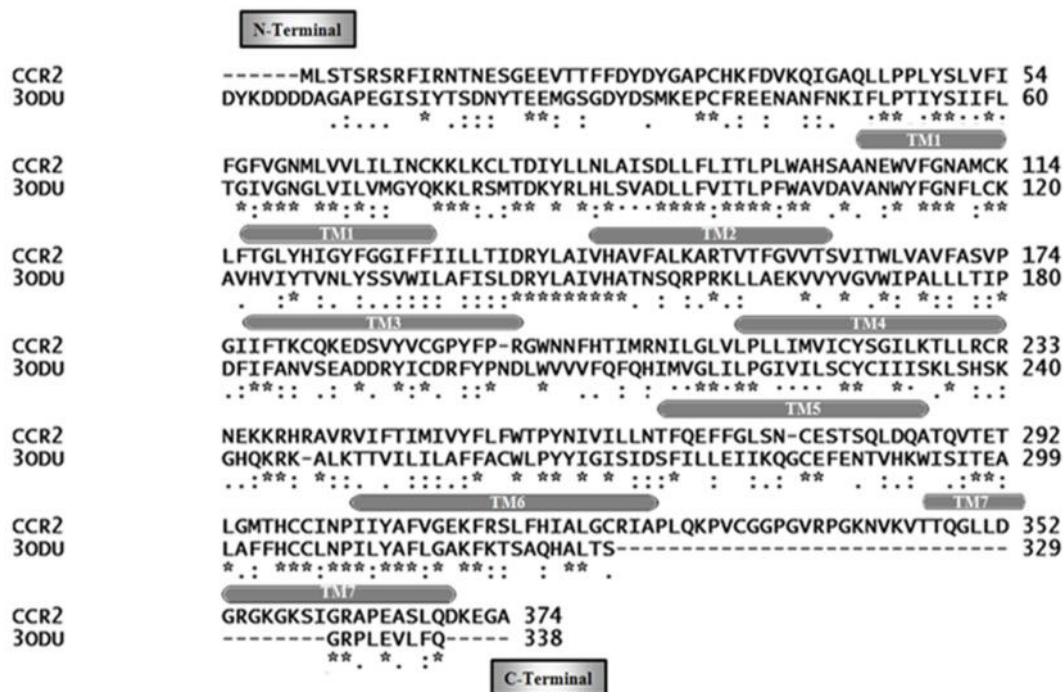


**Figure 1:** Alignment obtained between the query (CCR2) and template (PDB code: 3ODU) sequences for modeling. Identical residues are marked (\*), similar regions are marked (:). Secondary structure (TM domains) of the CCR2 receptor is indicated below the sequence in a cylindrical shape.

### **3.2. Homology modeling of CCR2**

CXCR4 (A chain) was used to develop the 3D models and a modeler program was used to derive 3D-models of CCR2. The unique feature of GPCR's is the presence of seven transmembrane helices. As CCR2 is also a GPCR, we introspect whether the seven transmembrane (TM) helices were properly transformed to the models according to that of the template (PDB code: 3ODU) structure. Fifty models were developed for CCR2 and finally the model with the lowest MolPdf as well as with the lowest RMSD compared with the template structure was selected for further computational analysis. The key factor in CC chemokines is the presence of disulphide bridges between conserved cysteines residues and more than 90% of the members of the GPCR super family have conserved disulfide bridges. Since the template structure also has the disulphide bridges in it, we checked whether the selected model has the disulphide bridges in it. As in template, we found that the disulfide bridges were produced between Cys32-Cys277 and Cys113-Cys190 of the selected CCR2 model. The model (CCR2) selected was further refined by simple energy minimization in vacuum, and the energy minimized CCR2 model using MDS is shown in Figure 2.

The model was further validated using Ramachandran plot of PROCHECK (40) to visualize the backbone dihedral angles against of amino acid residues in the selected protein structure. The Ramachandran plot for the CCR2 model showed that most of the residues were in favored (92.9 %) and in the additionally allowed (7.1 %) region. It is evident that, almost all models developed using modeling software pass the

PROCHECK validation regardless of model quality. This is because PROCHECK uses the criteria of visualizing backbone dihedral angles against the angles of amino acid residues in the protein structure, and thus, is more relevant for X-ray crystallographic studies. When the template and target structures are dissimilar, more caution should be taken and additional validation criteria must be used to determine the quality of the developed model.

Accordingly, additional parameters, such as, ERRAT (41) and Prosa (<https://prosa.services.came.sbg.ac.at/prosa.php>) energy plots were used to check the quality of the model. ERRAT plot is a program for verifying protein structures. Error values are plotted as a function of the position of a sliding 9-residue window. The error function is based on the statistics of non-bonded atomic interactions between atom types. Models with higher ERRAT scores are of higher quality, and the ERRAT score for CCR2 was found to be 87.04. Similarly, we validated our models using Prosa, which evaluates the energy of the structure using distance pair potentials. Residues with a negative Prosa score confirm model reliability. The Prosa energy scores for the template was -2.34 and for the model (CCR2) was - 2.54. High ERRAT scores and low Prosa energy scores indicate that models are of high quality. Overall, our results indicate the selected models were satisfactory. Ramachandran and Prosa energy plots for refined CCR2 model are shown in Figure 3a and Figure 3b. This refined and validated model of CCR2 was used for docking analyses.



**Figure 2:** Homology model (green) of CCR2 obtained and its refinement by MDS superimposed on the template structure CXCR4 (red).



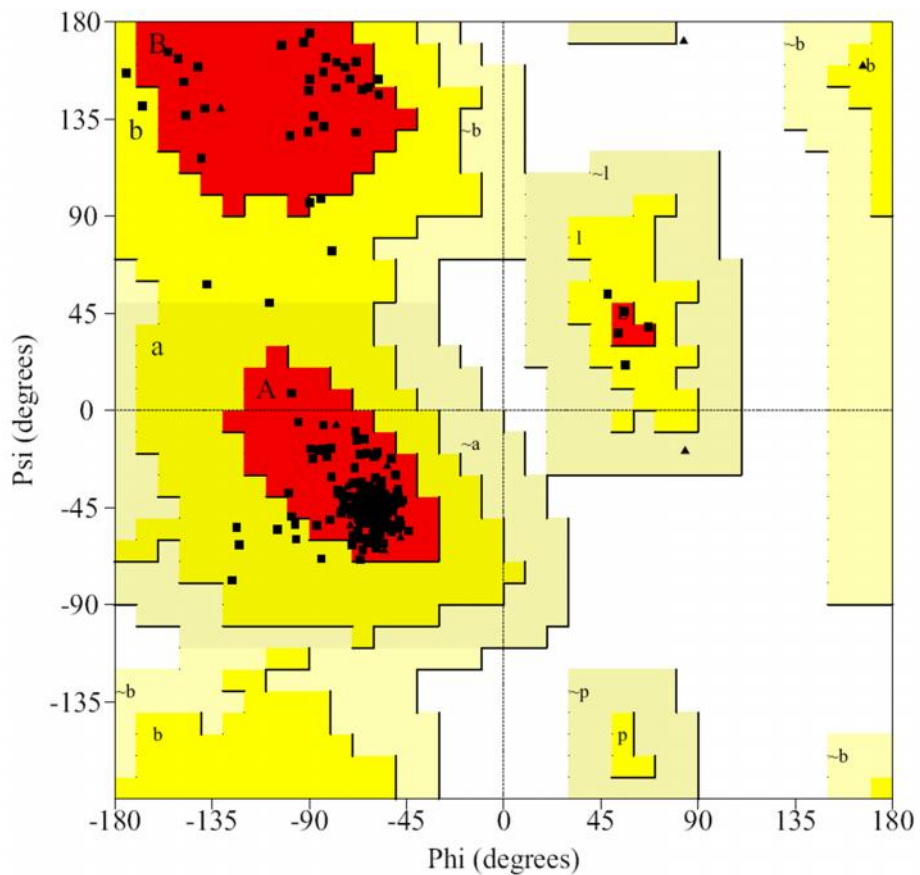


**Figure 3a:** Ramachandran plot of the developed CCR2 model refined by MDS. Different color codes indicate most favored (red), generously allowed (dark yellow), additionally allowed (light yellow), and disallowed (white) regions.

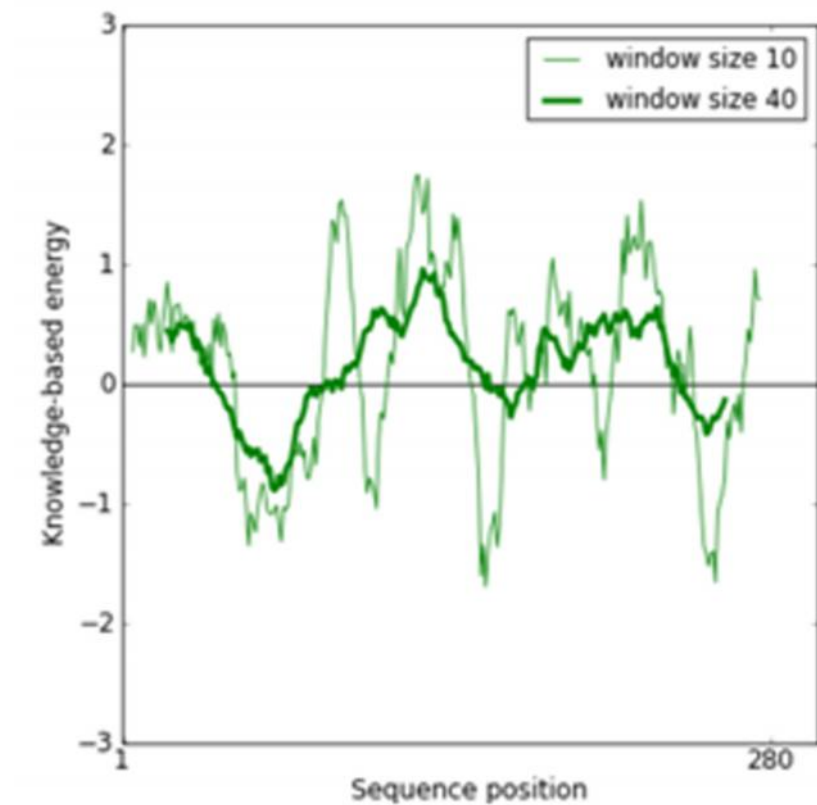


**Figure 3b:** Prosa energy plot for the developed CCR2 model refined by MD simulation.

### **3.3. Prediction of interaction between potent 4AAC antagonist and CCR2 receptor**

#### **3.3.1 Binding site of CCR2**

A putative binding site of CCR2 was determined as described previously (6 and 26). Previous receptor homology modeling suggests that CCR2 antagonists bind to an extended pocket bounded by TM2, TM3, TM5, TM6, and TM7 (56). Furthermore, it has been proposed in mutagenesis studies that Glu291 of TM7 is an important residue in the binding pocket (6 and 26). With knowledge of these previously published results, the binding pocket was determined. The binding pocket was found to be composed mainly of residues Leu45, Tyr49, Trp98, Ser101, Ala102, Tyr120, His121, Tyr124, Phe125, Met205, Arg206, Asn207, Trp256, Tyr259, Gln288, Glu291, Thr292, and Met295, which compares well with previous studies (6 and 26). The residues that in the binding pocket that guide docking are shown in Figure 4a (front view) and Figure 4b (top view).

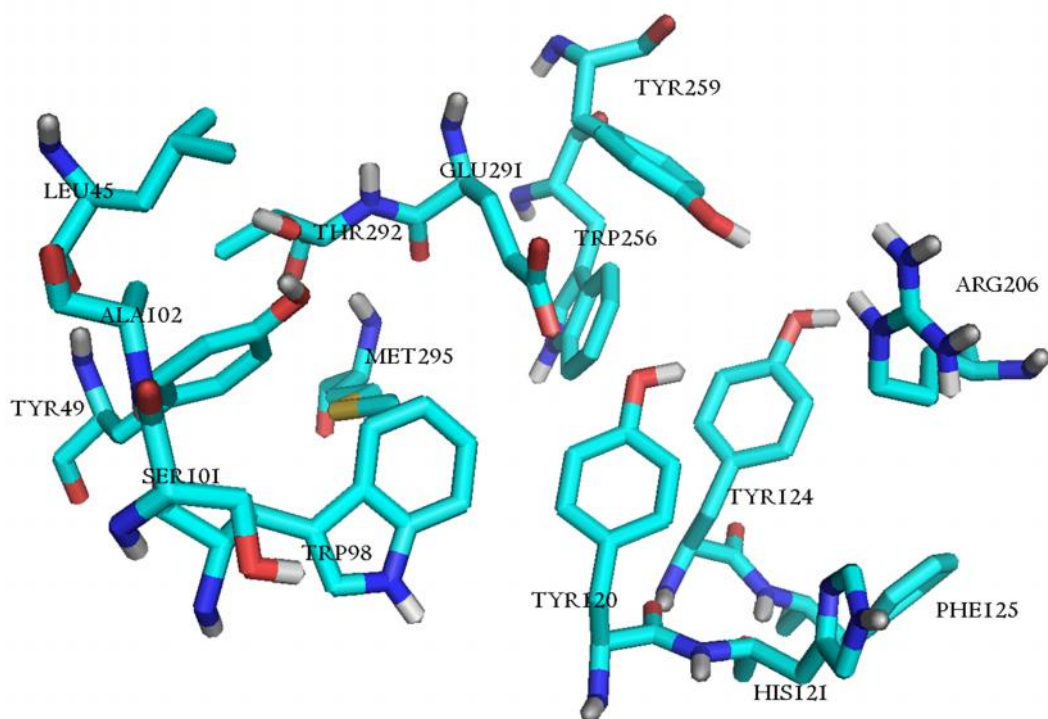


**Figure 4a:** Front view of the proposed binding pocket (CCR2). Binding site residues are colored based on atom types. Figure generated using the Pymol program (<http://www.pymol.org>).

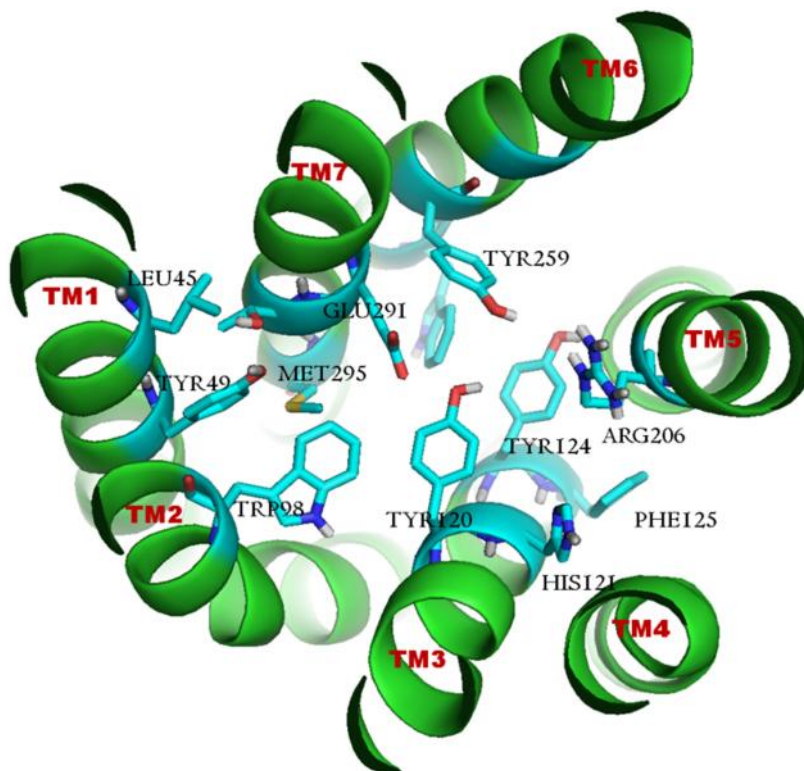


**Figure 4b:** Top view of the CCR2 binding pocket. Transmembrane (TM) helices are colored green, whereas the constructed binding pocket residues were color-coded with different colors depending on atom types. All TM regions are labeled in red on the tops of helices. Figure generated using the Pymol program (<http://www.pymol.org>).

### **3.3.2 Docking studies of highly active CCR2 antagonist (compound 16b of 4AAC)**

A series of highly active CCR2 antagonists have been reported by Zhang et al. (42). As the binding pocket projected in this study is similar to that of the previously published reports by Mirzadegan et. al. and Marshal et. al. (6 and 26), one of the potent CCR2 antagonist reported by Zhang ( $IC_{50} = 5$  nM,  $pIC_{50} = 8.3$ ) was docked into the binding site. Fifty conformations were generated and the top ranking conformational clusters from our docking study were evaluated. The conformations within the top ranked cluster were then selected for analysis. It was further observed that the selected cluster consists of 14 conformations within the cluster. It is well known that the top scoring binding mode is not always the correct binding mode in docking runs, even when ligands were docked into their own x-ray crystal structure. In cross docking experiments the top binding mode is rarely the native binding conformation. Docking against homology models makes it even more unlikely that the highest scoring pose is actually the correct pose. So, we carefully analyzed the conformations within the top cluster and two conformations were selected based on scoring function, interaction with crucial amino acid residues and salt bridge contact with Glu291.

The compound 16b of 4AAC bound with a binding energy of -8.95 kcal / mol and an intermolecular energy of -10.34 kcal / mol. In addition, the ligand established crucial interactions with important residues in the CCR2 binding site. The basic nitrogen in the azetidiny ring formed an electrostatic interaction (i.e., salt bridge

contact) with crucial and conserved Glu291, and the distance between the glutamic acid residue and the basic nitrogen was 4 Å. Furthermore, it was observed that the ligand formed hydrogen bond interactions. The hydrogen atom of amine nitrogen next to the azetidyl ring hydrogen bonded with Tyr49 and amine nitrogen close to the indazole ring of 4AAC hydrogen bonded with Trp98 at a distance of 2.4 Å. Moreover, the nitrogen of the indazole ring hydrogen bonded with Ser101 at a distance of 2.9 Å. In addition to the hydrogen bonds and salt bridge interaction, we looked for the residues which are in the vicinity of ligand. We found that residues, such as, Lys34, Leu45, Trp98, Ala99, Ala102, Trp106, Phe116, Val189, Cys190, Asn199, Thr203, Arg206, Asn266, Gln269, Asp284, Thr287, and Gln288 are in the vicinity of ligand (within 4Å from the ligand molecule). The docked mode of the ligand molecule and its interaction with active site residues is shown in Figure 5a.

In addition we also selected another binding mode to validate the stability of the binding mode using MDS. It would be also critical while analyzing the SAR's. It was observed that the ligand bound with a binding energy of -7.88 kcal / mol and an intermolecular energy of -8.4 kcal / mol. As the salt bridge distance between the ligand and Glu291 is crucial, we selected the pose with larger distance between them. Moreover, this binding mode shared the similar ligand space which is more or less similar to the previous mode with a slight variation in its orientation of substitutions. The docked mode of the ligand molecule and its interaction with active site residues is shown in Figure 5b.

Despite the fact that the binding modes selected in the present study and the interaction between 4AAC and CCR2 are similar to previous results, the present study may be limited because our selection of binding mode was based on the top cluster, previous mutagenesis results, and binding energy. This study can also be done manually by assigning the salt bridge contact as the starting point of interaction between the ligand and Glu291 residue as it is crucial for activity (6 and 26). However, our selected docked modes obtained the essential salt bridge contact with Glu291 with additional hydrogen bonds and also identified the residues in the TM1, TM2, TM3 and TM7 with additional residues from TM5 and TM6 as proposed by P.H. Carter and A.J. Tebben (56). These findings encouraged the reliability of our results.



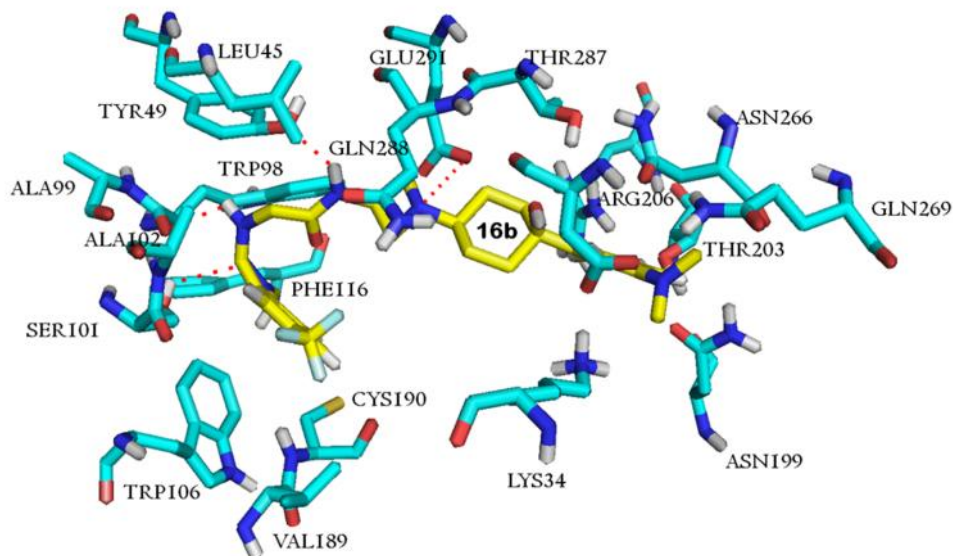


**Figure 5a:** Docked mode of compound 16b inside the proposed binding pocket of CCR2. Front view of the docked conformation of 16b. Binding site residues (carbon cyan, nitrogen blue and oxygen red) and the ligand molecule (carbon yellow, nitrogen blue and oxygen red) are colored based on atom types. Figure generated using the Pymol program (<http://www.pymol.org>).

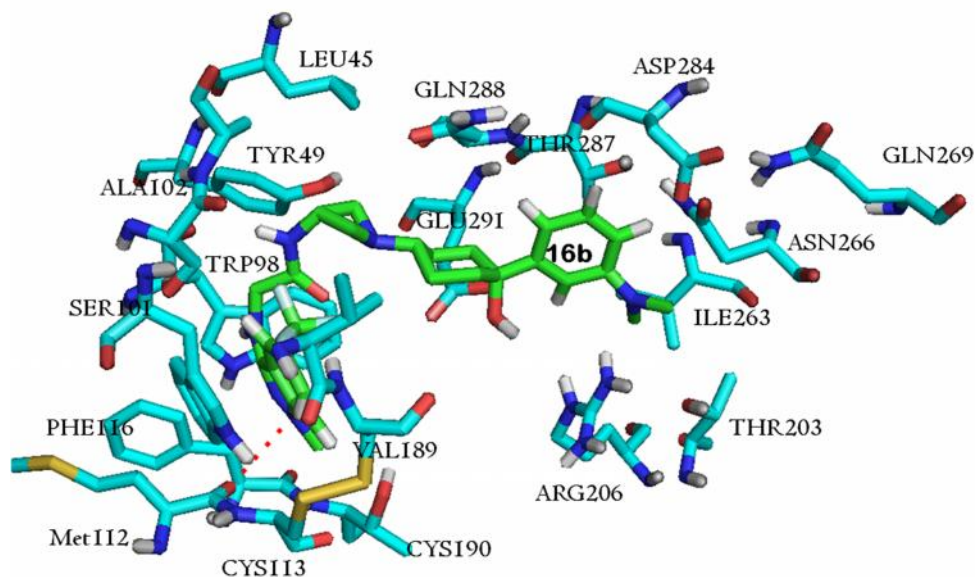


**Figure 5b:** Alternative binding mode of compound 16b inside the proposed binding pocket of CCR2. Front view of the docked conformation of 16b. Binding site residues (carbon cyan, nitrogen blue and oxygen red) and the ligand molecule (carbon yellow, nitrogen blue and oxygen red) are colored based on atom types. Figure generated using the Pymol program (<http://www.pymol.org>).

### **3.4. Molecular dynamics simulation of Receptor-Ligand-Membrane complexes**

Since CCR2 is a membrane protein, an accurate computational representation of CCR2 receptor should be embedded in a membrane aqueous environment. In vivo binding of inhibitor to a receptor is a dynamic process, where the docked orientation of ligand considers the receptor to be rigid. To overcome the bias more relevantly, molecular dynamics simulation of CCR2-ligand (selected poses from docking) complex embedded in a lipid layer was done to mimic the real biological environment. Accordingly, we analyzed a membrane MD simulation of the docked model of one of the 4AAC derivatives complexed with CCR2. This strategy employed here could help us to identify the most stable and low energy conformation of CCR2-4AAC complex. We assume the selected conformation of ligand inside the receptor could be the bioactive one. As the rest of the molecules in the dataset have similar core structure and variations in only substitutions, by assuming the stable and average conformation of ligand-receptor complex as the bioactive one, it will allow us to understand the SAR's of 4-azetidiny-1-aryl-cyclohexane derivatives. Furthermore, the SAR's of diverse CCR2 ligands could be analyzed in the same manner to obtain additional insights of the CCR2 binding site. In addition, the model obtained and relaxed in the membrane environment could be more appropriate for the structure based design of novel CCR2 antagonists.

### **3.4.1 Setting up of CCR2-16b of 4AAC-lipid for the production run**

The selected docked conformations of 16b of 4AAC complexed with CCR2 were implanted in a rectangular box composed of a DPPC bilayer solvated with water molecules. Overlapping lipids were deleted. It has been observed that, three lipid molecules from the upper leaflet and three lipid molecules from the lower leaflet were deleted using InflateGRO. After the deletion of overlapping lipids, the protein-ligand-lipid complex was then shrunk until it reaches an area per lipid of  $0.65 \text{ \AA}^2$ , which is closest to the reference value for DPPC lipids. The protein-ligand-lipid complex was then solvated by adding water molecules and appropriate counter ions [27 Na<sup>+</sup> and 37 Cl<sup>-</sup>] were added to neutralize the system. To overcome the structural artifacts, the system was then energy minimized. The system composed of protein, ligand, lipids, water molecules and ions was then equilibrated and a final production run of 20ns was performed. The tightly packed, prepared system (CCR2-16b of 4AAC-lipids-water molecules) included in the production run is shown in Figure 6.

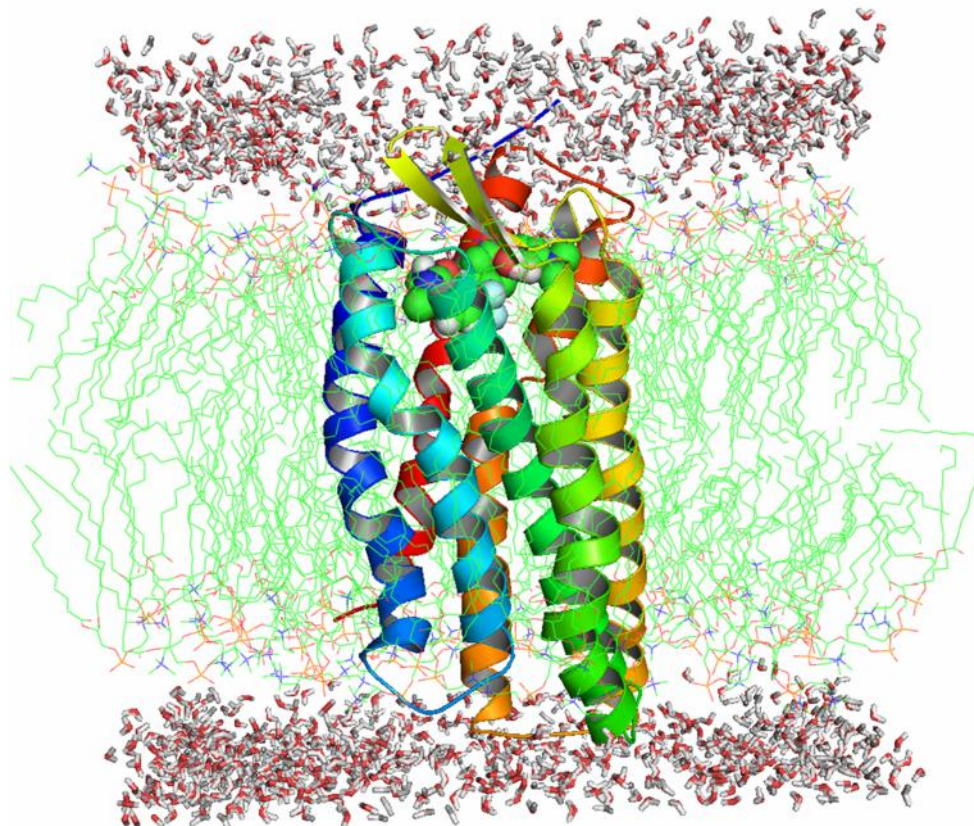


**Figure 6:** Side view of CCR2-ligand-membrane-aqueous environment for a production runs of 20 ns MDS. Seven transmembrane helices are represented as cartoons, the ligand molecule as a surface, lipid molecules as lines, and water molecules as sticks. Figure generated using the Pymol program (<http://www.pymol.org>).

### **3.4.2 Structural analysis of CCR2-4AAC complexes throughout production runs**

A number of parameters needed to be examined to substantiate the physical stability of the CCR2 model. The stability of the system was examined structurally and energetically during MD simulation as a function of time. The total energy and root-mean square deviations of protein structure versus initial structure were used as parameters to monitor the stability of the model. The total energy plot of the system indicated that the total energy decreased gradually until 3 ns and then stabilized at this level. Trajectory based analysis revealed the total energy of the system decreased from  $-1.81 \times 10^5$  KJ/mol to  $-2.16 \times 10^5$  KJ/mol. It was observed that most of the structures are around  $-2.14 \times 10^5$  KJ/mol, indicating the system were energetically stable. The CCR2 model was also evaluated on the basis of structural stability using RMSD calculated by structural variations with respect to time; the initial period was considered as period of equilibration. A gradual rise in RMSD until 0.38 nm (1.17 ns) and then decreased gradually to 0.34 nm till 5ns. This was then followed by a plateau, which for most of the structures occurred at around  $0.34 (\pm 0.02)$  nm till 20 ns. These results indicated the structural stability of the model. The RMSD of ligand molecule and the movement of ligand atoms throughout the simulation were also analyzed. It was observed that the initial conformation gradually moved to  $0.2 (+0.2)$  nm till 2ns, and then gradually decreased to 0.16 ns around 3.9ns. This was then followed by a slight increase in its rmsd and reached 0.2 nm around 6ns and maintained around  $0.2 (\pm 0.02)$  nm till 20ns.

These results suggest that this ligand is stable throughout the simulation. The total energy plot and the RMSD plot of the receptor and ligand molecules are shown in Figures 7a, 7b, and 7c, respectively.

It was observed from our initial docking study that the selected binding mode was based on previous results and crucial interaction with active site residues. Moreover, further MD simulation study found that the selected binding mode was found be stable structurally as well as energetically. However it is well known fact that the top scoring binding mode is not always the correct binding mode. Though our selected binding mode was based on scoring function, salt bridge contact and crucial interactions, to overcome the bias and to validate the selection of binding mode another binding mode was implemented for 20ns MDS. The rmsd plot of ligand molecule indicates that the ligand is moving throughout the production run and found to be unstable (Figure 8b). Moreover the movement of ligand molecule makes the protein structure to be unstable and the rmsd continues to rise throughout the simulation (Figure 8a). These results validate the selection of binding mode.

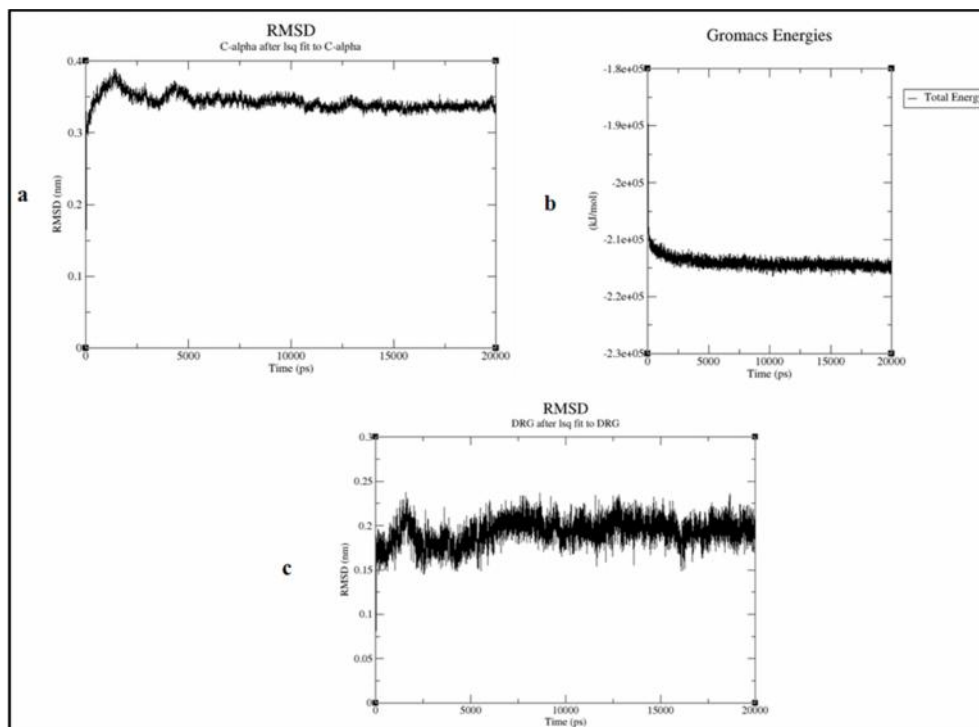


**Figure 7:** (a) Total energy plot of the MD simulation and variations in system total energy over 20 ns. (b) Root mean square deviation (RMSD) plot for CCR2 C from initial structures throughout the 20 ns simulation as a function of time. (c) Root mean square deviation (RMSD) plot for DRG as ligand throughout the 20 ns simulation.



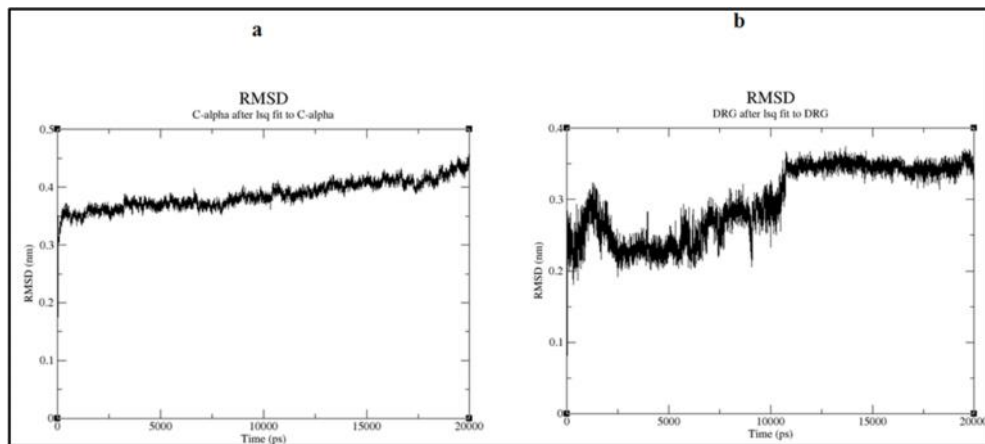


**Figure 8:** (a) Root mean square deviation (RMSD) plot for CCR2 C from initial structures throughout the 20 ns simulation as a function of time. (b) Root mean square deviation (RMSD) plot for DRG as ligand throughout the 20 ns simulation.

### **3.4.3 Binding mode (CCR2-16b of 4AAC) and trajectory analysis**

It was observed from the RMSD plot of ligand molecule that, the ligand was moved from initial position inside the proposed binding site and it maintained around  $0.2 \pm 0.02$  nm after the equilibration period. Our results indicate the practical relevance of molecular dynamics simulation after initial rigid docking analysis inside proposed binding site. The selected docked mode after initial rigid docking observed that, the ligand established hydrogen bonding with Tyr49, Trp98 and Ser101 and moreover the salt bridge distance is 4 Å (Figure 5a). However, the binding mode of 4AAC in the binding pocket of CCR2 (Figure 9), which were derived from the average low energy structure from MD simulation leads to introduction of some new residues and some new interactions into the binding pocket compared with docking. There are some differences in interaction of 4AAC, and these differences somewhat affect the position of ligand molecule in the binding pocket of CCR2. We did monitored the detailed protein-ligand interaction over time through minimum distance analyses between important residues, salt bridge distance between crucial Glu291 and basic nitrogen in the azetidiny ring of ligand molecule.

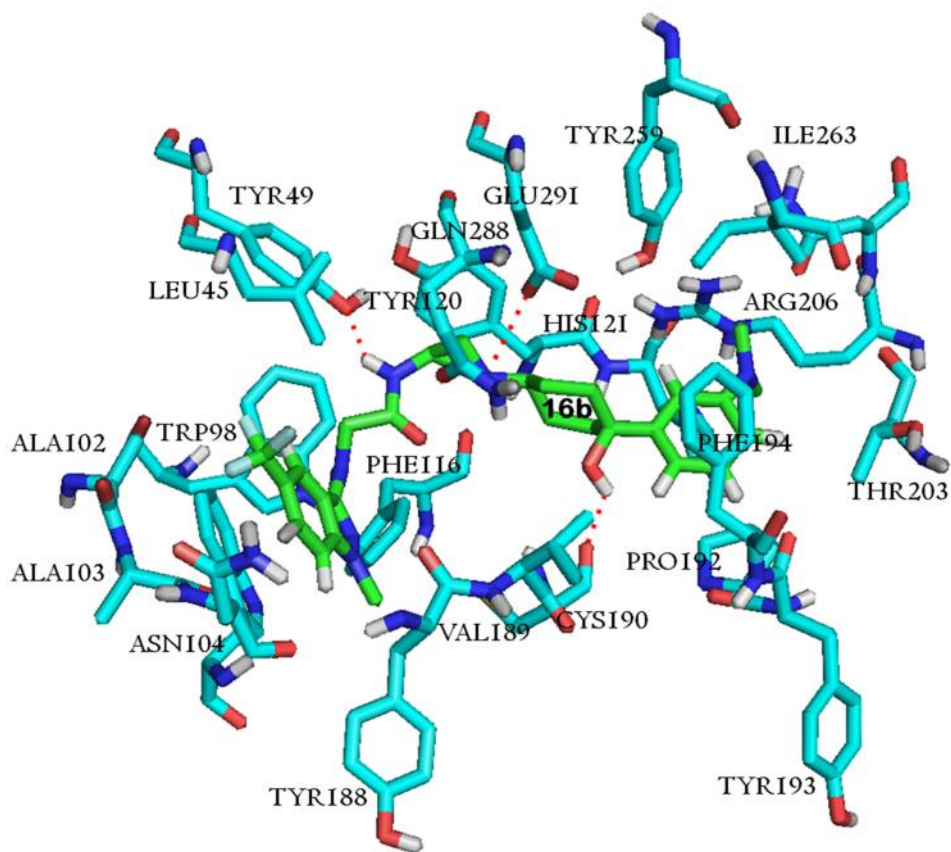


**Figure 9:** Front view of the docked mode of compound 16b inside the proposed binding pocket of CCR2 after MDS. Binding site residues (carbon cyan, nitrogen blue and oxygen red) and the ligand molecule (carbon yellow, nitrogen blue and oxygen red) are colored according to atom type.

In the case of binding mode of 16b inside the CCR2 binding pocket (average low energy structure) derived from MD simulation, some new residues were noted in vicinity of the ligand. Our analysis of the 20 ns MDS of the interaction between CCR2 and the 16b of 4AAC revealed additional residues, such as, Ala103, Asn104, Tyr120, His121, Tyr188, Val189, Cys190, Pro192, Tyr193, Phe194, Asn207, Ty259 and Ile263 moved into the vicinity of ligand (within 4 Å). More importantly, the hydrogen bonding between the ligand and Ser101 obtained from initial docking vanished after MDS, suggesting that this bonding might not be crucial and not in vicinity of the ligand. However, Tyr49, which hydrogen bonds with 16b of 4AAC, was found to stay in the vicinity of the ligand, which confirms the importance of this residue suggested by previous mutational studies. The hydrogen bond between Trp98 and 16b after initial docking got vanished because of the ligand movement; however this residue stayed in vicinity throughout the simulation which confirms the importance of the residue. The distance between residues (Tyr49, Trp98 and Ser101) and 16b was monitored throughout the simulation and shown in Figure 10.

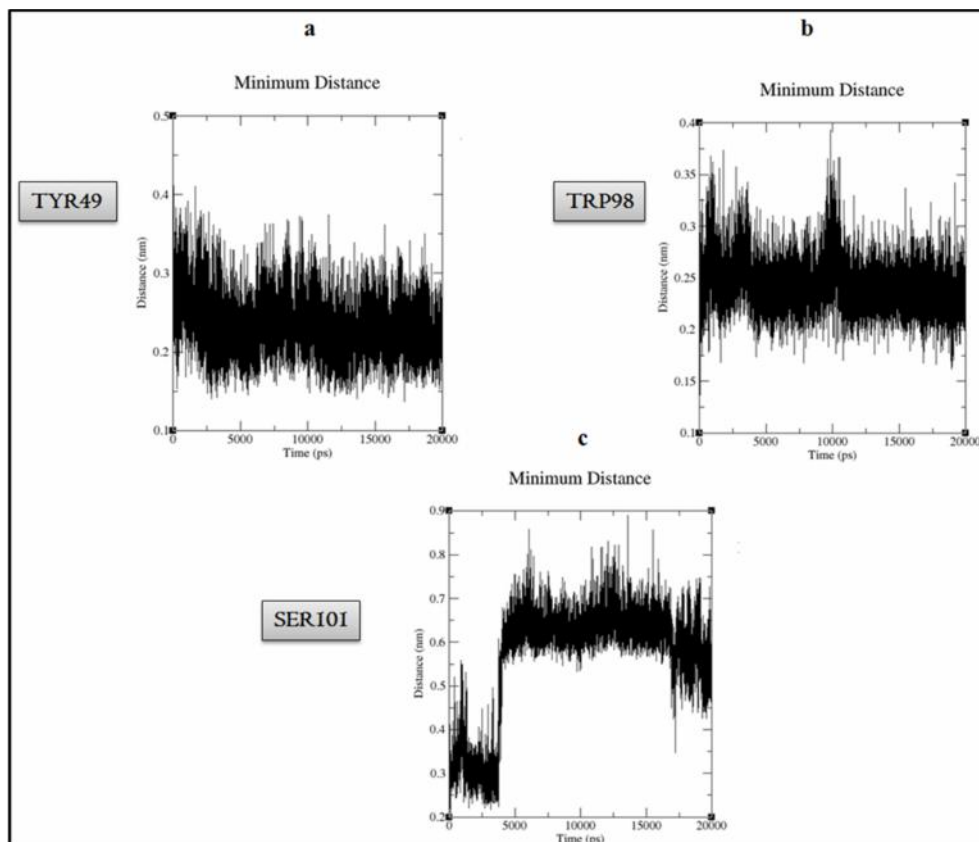


**Figure 10:** Minimum distances between the 16b and CCR2 active site residues surrounding 4 Å were computed using MD simulation trajectories. (a) Tyr49 and 16b, (b) Trp98 and 16b and (c) Ser101 and 16b. Minimum distances were calculated and plotted as a function of time.

Similarly, the initial distance between the glutamic acid residue and the basic nitrogen in the azetidiny ring was found to be 4 Å (i.e., salt bridge contact). The distance between them in the average structure after MDS was found to be 3.5 Å. It revealed the presence of a strong electrostatic interaction. The results of the present study show the importance of this interaction for activity and complement previous results. The distance between Glu291 and basic nitrogen of azetidiny ring throughout the simulation is also plotted and is shown in Figure 11. It was also observed that Tyr120 and His121 were not in the vicinity of ligand in the initial docked mode. However, these residues are back in vicinity and suggested the importance of these residues and complements previous mutational studies (Figure 12).

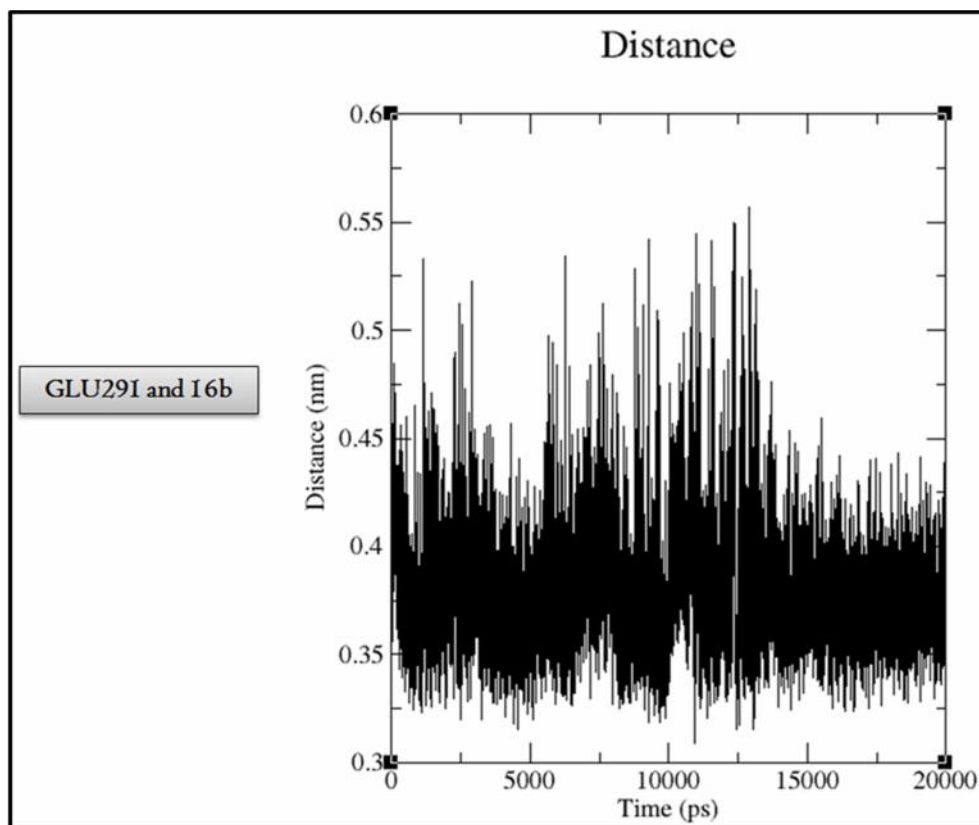


**Figure 11:** Minimum distances between Glu291 (Oxygen atom) and 16b (basic nitrogen in azetidiny ring) computed using MD simulation trajectories. Minimum distances were calculated and plotted as a function of time.

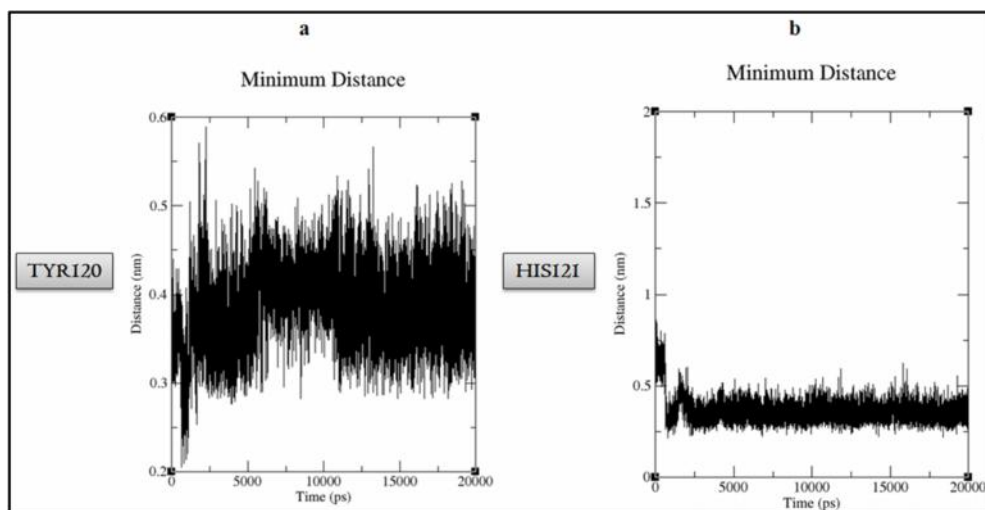


**Figure 12:** Minimum distances between (a) Tyr120 and 16b and (b) His121 and 16b.

Minimum distances were calculated and plotted as a function of time.



The indazole ring of 16b moved inside the pocket lined by mostly hydrophobic residues such as Trp98, Trp106, Phe116 and Tyr188. This interaction stabilized the position of ligand inside the pocket. The hydroxyl group of the cyclohexyl ring, hydrogen bonded with Cys190. Moreover, the N-methyl of the R1 substituted phenyl ring oriented towards Thr203, Arg206 and Asn207, implying the importance's of these residues and suggesting the need for mutational studies. The minimum distance between these residues and 16b was also monitored and shown in Figure 13. Residues such as Tyr259 and Ile263 which was not in vicinity after initial docking moved towards the ligand and mutational studies on these residues could also be effective. The distance between these residues and 16b was also been monitored throughout the simulation and shown in Figure 14. On the contrary, residues such as Lys34, Ala99, and Ser101 moved out of ligand's vicinity during the course of simulation.

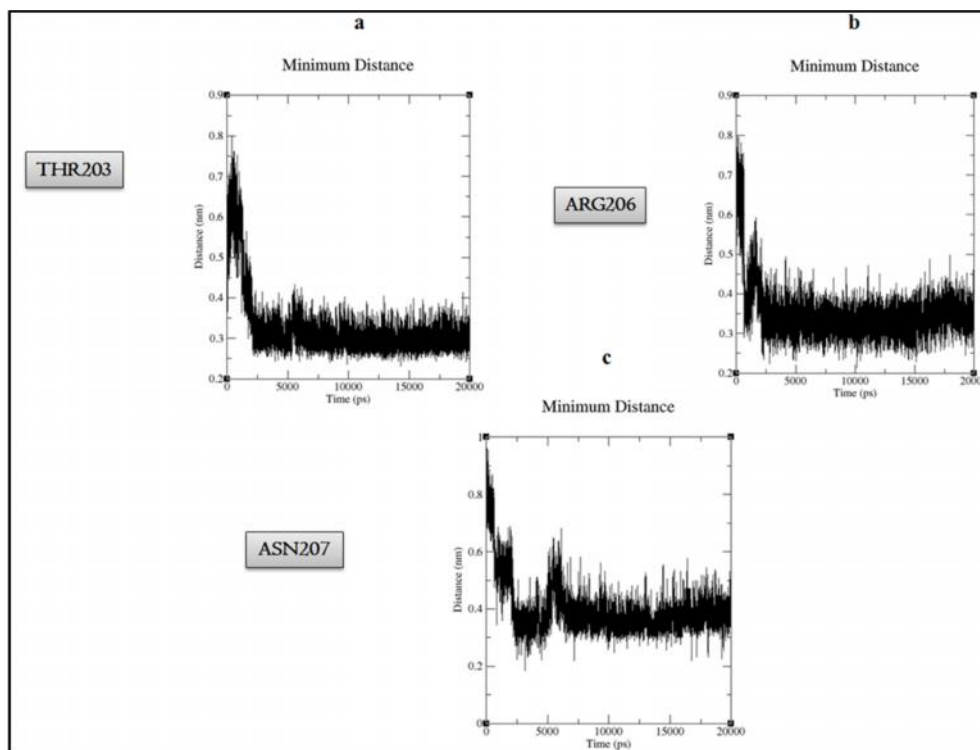


**Figure 13:** Minimum distances between (a) Thr203 and 16b, (b) Arg206 and 16b and (c) Asn207 and 16b. Minimum distances were calculated and plotted as a function of time.

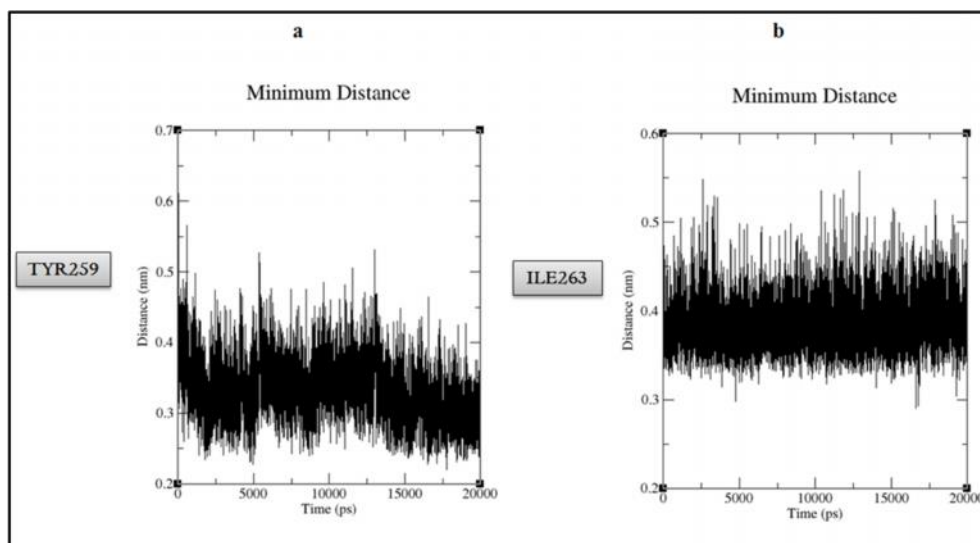


**Figure 14:** Minimum distances between (a) Tyr259 and 16b and (b) Ile263 and 16b. Minimum distances were calculated and plotted as a function of time.

### 3.4.4 SAR studies of 4-azetidiny-1-aryl-cyclohexane derivatives

The average low energy structure (CCR2-ligand) resulted from the MD run was further used to exploit the SAR's of 4AAC derivatives. We considered the binding mode of 16b from 4AAC ( $IC_{50} = 5$  nM,  $pIC_{50} = 8.3$ ) resulted from MDS as a bioactive conformer and the representative molecule for other 4-azetidiny-1-aryl-cyclohexane derivatives reported by Zhang et al. We then compared the binding mode of this compound with those of the other molecules, since other molecules in the dataset are similar with varied substitution and SAR's were explored.

Our trajectory analysis and the binding mode of 16b from the average structure indicated that the basic nitrogen is necessary for activity, because of its electrostatic interaction with Glu291 in the binding site. It was also evident that compounds with hydrophobic substitution around R1 enhance activity, and that optimal bulky substitution at the R1 substituted phenyl ring is needed for activity and that the 1-hydroxyl groups of the cyclohexyl ring enhances activity. These SAR's explain the greater activities of compounds 13b ( $IC_{50} = 6$  nM,  $pIC_{50} = 8.2$ ), 16e ( $IC_{50} = 6$  nM,  $pIC_{50} = 8.2$ ), 16h ( $IC_{50} = 7$  nM,  $pIC_{50} = 8.1$ ), and 16b ( $IC_{50} = 5$  nM,  $pIC_{50} = 8.3$ ). Compounds from series 14 (14a, 4b, 14c, 14e, 14f, 14j, 14k, 14m, 14n) were not active because they lacked desirable hydrophobic substitution at R1. Similarly compounds, such as, 16q ( $IC_{50} = 480$  nM,  $pIC_{50} = 6.3$ ), 16r ( $IC_{50} = 1400$  nM,  $pIC_{50} = 5.8$ ) and 16t ( $IC_{50} = 10000$  nM,  $pIC_{50} = 5$ ), which lack hydrophobic substitution at R1 had poor activities. On the other side of the 16b from 4AAC, an indazole ring is needed, and this hydrophobically

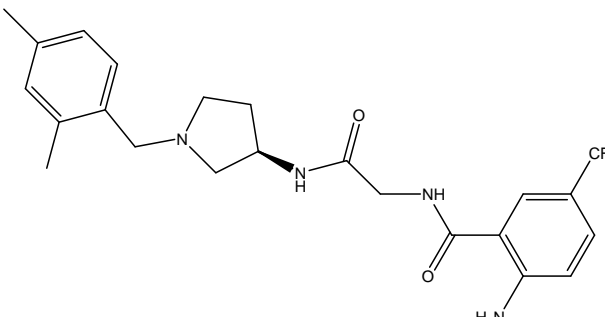
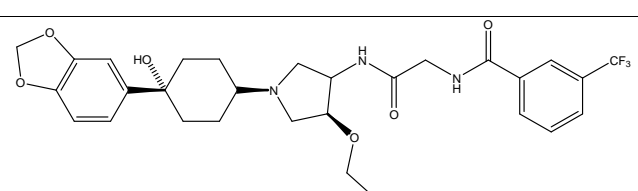
interacts with Trp98. The indazole ring is desirable to access the hydrophobic residues Ala102, Ala103, Trp106, Phe116, Tyr188, and Val189 in the CCR2 binding pocket. Though compounds such as 13g, 13h, 14q, 14r, 14s, 14t, 14u, 14v, 16l, 16m substituted with hydrophobic groups around R1 they lacked activity. The reason is because of increased substitution around the indazole ring which is sterically restricted to the receptor. Our analysis concluded that molecule with hydrophobic substitution around R1 and the optimal substitution around indazole is desirable for potent activity.

### **3.4.5 Comparison of other potent antagonists with the MD simulated model**

The selected low energy model obtained after a prolonged run for 20 ns MDS was considered to be stable enough to allow meaningful analyses of CCR2 binding site and CCR2 antagonists. We considered this more relaxed structure as a valid one and compared the binding site of CCR2 with some of the potent CCR2 antagonists. More appropriately, the orientation of crucial active site residues after MDS will help us to identify the possible orientation of some of the potent antagonists of CCR2. We then analyzed the binding mode of selected CCR2 antagonists based on its pharmacophore properties against some of the key residues in the active site. The importance of electrostatic interaction between Glu291 and the basic nitrogen in the ligand molecule was considered as the starting point. Although there could be some limitations with this approach, it could be useful in identifying the binding mode of some new antagonists.

Accordingly, we chose a representative set of potent CCR2 antagonists (Table 3). Initially, the pharmacophoric features of highly active compound 71 ( $IC_{50} = 3.2$  nM,  $pIC_{50} = 8.4$ ) of the Teijin lead (28) was compared with the binding site. The basic nitrogen in the pyrrolidine ring is probably forming an electrostatic interaction with Glu291. The 2,4-di-methyl-phenyl ring which is highly hydrophobic is expected to hydrophobically interact with hydrophobic pocket lined by residues Trp98, Ala102, Ala103, Trp106, Phe116, Tyr188, and Val189. The linear chain mediating the pyrrolidine ring and 2-NH<sub>2</sub>, 5-trifluoro methyl group might interact with Tyr120 and Tyr259. The 2-NH<sub>2</sub> of the phenyl ring may access the pocket lined by residues Thr203, Arg206 and Asn207. Similarly we examined the potent CCR2 antagonist, INCB3344 ( $IC_{50} = 10$  nM,  $pIC_{50} = 8$ ) originally identified by Brodmerkel et.al (57). This ligand is more or less similar to 16b of 4AAC and expected to occupy the same volume and probably with similar orientation. It was clear that Glu291 is a crucial residue and it supposed to form an electrostatic interaction with the basic nitrogen of ligand molecule. On account of this as the starting point and from the perspectives of binding site residues it is possible to identify the probable binding mode of some other potent CCR2 antagonists.

Table 3. Representative set of CCR2 antagonists to derive the binding mode from the perspectives of binding site

Compound	Structure	IC <sub>50</sub> (nm)	pIC <sub>50</sub>
Teijin Lead (Compound 71)		3.2	8.4
INCB3344		10	8

### **3.5. Comparative analysis of CCR2 and CCR5**

We compared the sequences of CCR2 and CCR5, and found 66% sequence identity. They also share 82% identity in their active sites. From the alignment (Figure 15) we found that the most of the residues are conserved. Since dual targeting of CCR2 and CCR5 is of prime importance in current drug discovery, we moved our focus towards the binding site of these receptors. We superimposed the binding sites of both receptors and analyzed the variation of residual information. Our analysis revealed that almost all the residues are identical except three residues. The varying residues in CCR2/CCR5 are Ser101/Tyr89, His121/Phe109, and Arg206/Ile198; these differ in their electrostatic properties. More specifically, Ser101 is hydrophilic and Tyr89 is hydrophobic in nature. Similarly, His121 and Arg206 are hydrophilic, whereas Phe109 and Ile198 are hydrophobic in nature. While designing dual inhibitors one may consider this variation of active sites residues for potent inhibition of dual targets. It will also help the researchers to consider the issue of selectivity to selectively inhibit CCR2/CCR5. Mutational studies on these residues could also be effective. The superimposed binding site of CCR2/CCR5 is shown in Figure 16.



```

CCR2 MLSTSRSRFIRNTNESGEEVTTFFDYDYGAPCHKFDVKQIGAQLLPPLYSLVFI FGFVGN 60
CCR5 -MDYQVSSPIYDIN-----YYTSEPCQKINVKQIAARLLPPLYSLVFI FGFVGN 48
      :. . * * * : *          * . **:*:***:*****:*****
      :. . * * * : *          * . **:*:***:*** ** :* ***:**:*:***

CCR2 MLVVLILINCKKIKCLTDIYLLNLAISDLLFLITLPLWAHSAANEWVFGNAMCKLFTGLY 120
CCR5 MLVILILINCKRLKSMTDIYLLNLAISDLFFLLTVPFWAHYAAAQWDFGNTMCQLLTGLY 108
      ***:*****:*:*****:*****:***:*:*:*** ** :* ***:**:*:***

CCR2 HIGYFGGIFFIILLTIDRYLAIVHAVFALKARTVTFGVVTSVITWLVAVFASVPGIIFTK 180
CCR5 FIGFFSGIFFIILLTIDRYLAVHAVFALKARTVTFGVVTSVITWVAVFASLPGIIFTR 168
      .**:*:*****:*****:*****:*****:*****:*****:*****:*****:

CCR2 CQKEDSVYVCGPYFPRG---WNNFHTIMRNILGLVPLLLIMVICYSGILKTLLRCRNEK 236
CCR5 SQKEGLHYTCSSHPYSQYQFWKNFQTLKIVILGLVPLLLVMVICYSGILKTLLRCRNEK 228
      .***. * *.:** . *:*:*: *****:*****:*****:*****

CCR2 KRHRAVRVIIFTIMIVYFLFWTPYNIIVLLNTFQEFFGLSNCESTSQLDQATQVTETLGMT 296
CCR5 KRHRAVRLIFTIMIVYFLWAPYNIIVLLNTFQEFFGLNCCSSNRLDQAMQVTETLGMT 288
      *****:*****:*****:*****:*****:*****:***:*:***** *****

CCR2 HCCINPIIYAFVGEKFRSLFHIALGCRAPLQKPVCGGPGVPRGKNVKVTTQGLLDGRGK 356
CCR5 HCCINPIIYAFVGEKFRNYLLVFFQKHIA---KRFC-----KCCSIFQ---EAPER 334
      *****:*****:*****:*****:*****:*****:*****:*****:*****:
      : : : :** *.* * .: * :. :

CCR2 GKSIGRAPEASLQDKEGA 374
CCR5 ASSVYTRSTGEQEISVGL 352
      ..*: . . . : . *
    
```

**Figure 15.** Alignment obtained between the CCR2 and CCR5 sequences for sequence analysis. Identical residues are marked as (\*), similar regions are marked as (:)

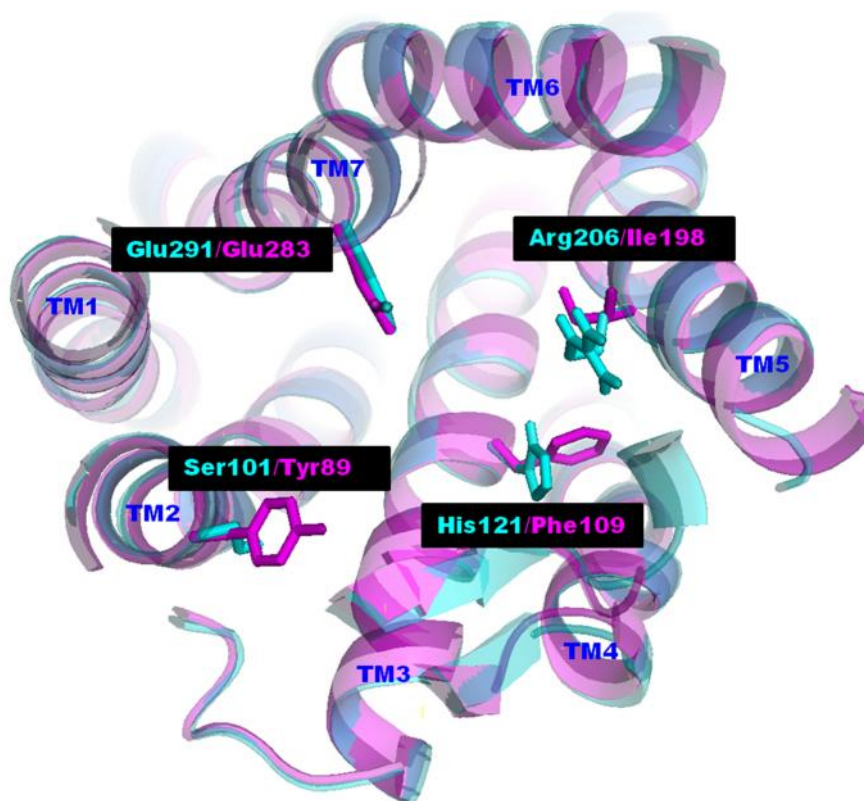


**Figure 16.** Superposition of varying residues in the active sites of CCR2 (cyan) and CCR5 (magenta). All the TM's are labeled by blue color on the top of helices.

## **4. Discussion**

CCR2 is a CC chemokine receptor and an important player in the trafficking of monocytes/macrophages. It also functions in cell types and is relevant during the pathogenesis of various diseases such as arthritis, multiple sclerosis, and type-2-diabetes (58), and thus CCR2 is considered an important receptor. Several research groups have studied the SAR's of CCR2 antagonists experimentally (28, 29 and 42) and computationally (30, 59 and 60). However, no study has been previously conducted on the time dependent interactions between CCR2 and antagonists using MDS. This paucity of data prompted us to undertake the present study to determine the effects of active site residues in the vicinity of ligand. More specifically, the objective of this study was to analyze the behavior of CCR2-4AAC complexes in a membrane environment and to characterize the reasons for antagonistic activity for some other antagonists (Teijin lead and INCB3344) from the perspective of binding site after MDS. Comparative analysis of CCR2/CCR5 binding sites was done to facilitate the development of dual antagonists and also to address the issue of selectivity.

As a starting point of this study, the homology model of CCR2 was developed. Previously homology models of CCR2 were developed using the traditionally used bovine rhodopsin and the recently reported  $\beta$ -adrenergic receptors as templates (26, 61-63). In this study by using more recently reported CXCR4 (PDB code: 3ODU) as a template structure, modeling was done because of the non-availability of crystal structure. Molecular docking study was then performed with 16b

of 4AAC against the proposed binding site (6, 26 and 27). One conformation was selected and the results are in line with previously published results. Glu291 has been previously established by mutational studies to be a crucial residue in terms of the activities of CCR2 antagonists (6, 26), and this is confirmed by our results, which show that Glu291 forms a salt bridge with antagonists at the active site. We also observed that hydrogen bonds were observed between the ligand and Tyr49, Trp98 and Ser101 of CCR2. These results are in line with previous mutagenesis studies (26, 64).

However, above the mentioned results obtained from the docking study are far from conclusive. Binding of an inhibitor to a receptor is a dynamic process, and the rigid docking results obtained can only represent instantaneous states, and thus, as only a glimpse of the possible molecular structures involved in docking. Nevertheless, dynamic ligand binding to receptor is more realistic and MDS studies can allow stable structures and better binding modes to be identified. Thus, in the present study, we performed membrane MDS to better understand the SAR relations between CCR2 and 4-azetidiny-1-aryl-cyclohexane derivatives. We consider that the relaxed model derived in a membrane environment is probably more appropriate for the structure based drug design of novel CCR2 antagonists.

As sampling protein dynamics in a single, 20 ns MD run is rather short by today standards we pointed out the limitations arising from the small amount conformational sampling and are as follows. It could happen that the short simulation time could not allow interacting protein-ligand at their full performance. In some cases

ligand binding could result in protein folding or structural changes with long runtime simulation, which could not be possible with small simulation time. Short runtime simulation shows variable RMSD throughout simulation. In contrast long runtime simulation allows protein to stabilize its coordinates and proper folding. Different conformation of ligand can be observed in short as well as long time simulations. Inadequate conformational sampling can be done in short time simulations. More typically, the ligand may bind and stabilize only a subset of the many conformations sampled by its dynamic receptor, causing the population of all possible conformations to shift towards those that can best accommodate binding. Beyond these limitations, this study is helpful in identifying the crucial residues, binding site movement, position of ligand and interaction of ligand with crucial residues which is quite encouraging.

The MDS analysis performed in the present study provides crucial insights of the character of the CCR2 binding site. The hydrogen bond between Ser101 and the 16b of 4AAC vanished and the ligand moved towards the hydrophobic residues Trp98, Ala102, Ala103, Trp106, Phe116, Tyr188, and Val189. However, the hydrogen between Tyr49 was retained and it was maintained during MDS. More importantly, the distance between Glu291 and the basic nitrogen in azetidiny ring decreased from 4 Å (before MDS) to 3.5 Å (after MDS). Furthermore, the N-methyl of the R1 substituted phenyl ring oriented towards Thr203, Arg206 and Asn207, implying the importance's of these residues and suggesting the need for mutational studies. Overall, we found that Tyr49, Trp98, Tyr120, and Glu291 are crucial for activity, which concurs with previous

mutagenesis results (6, 26 and 64). In addition, we found that Ala102, Thr203, Arg206, Asn207 and Tyr259 are probably crucially required for activity, and we believe that this warrants further mutagenesis studies.

Our SAR studies showed that electrostatic interaction between 4AAC derivatives and Glu291 is highly desirable, and that hydrophobic substitution of the cyclohexyl ring (R1 substitution) is required. Furthermore, optimal substitution around the indazole ring is required for better activity and bulky substitution hampers activity due to steric effects. In addition, we examined Teijin and INCB3344 (both potent CCR2 antagonists) with respect to binding by MDS. Our results could also be helpful in determining the binding mode of new antagonists.

We have been working on chemokine receptors using in silico methodologies (30, 65 and 66). In particular, we have developed 3D-QSAR models for CCR2 using ligand based and receptor guided methodologies (30). In this study, we used Teijin derivatives (28) to derive CoMFA and CoMSIA models, and we found that Ala102 and Asn207 are probably crucial for activity. More recently, we compared the binding sites of CCR2 and CCR5 to facilitate the development of dual antagonists targeting both CCR2 and CCR5 (65). In the present study, we found that Ser101 are important for CCR2 antagonism from our initial rigid docking study. However, the dynamic process showed that 4AAC derivative moved away from Ser101 and the hydrogen bond vanished. N-di-methyl substitution moved toward the region lined by residues Thr203, Arg206, and Asn207 whereas other residues, such as, Ala102, Thr203, and Arg206

stayed in the vicinity of the ligand (within 4 Å). These findings suggest the results obtained are realistic and that mutational studies on these residues are warranted.

## **5. Conclusion**

In the present study, the time-dependent behavior of CCR2/4-azetidiny-1-aryl-cyclohexane derivative complexes was studied by molecular dynamics simulation. CCR2 is a key player in monocyte trafficking and also has cell-dependent functions relevant to the pathogenesis various diseases. In silico methodologies, such as, comparative modeling, docking, and molecular dynamics simulation studies (20 ns) were performed in an explicit lipid layer environment. Homology modeling was performed using CXCR4 as template. Docking of 4-azetidiny-1-aryl-cyclohexane derivative at the proposed CCR2 binding site was performed. MDS was then performed with the docked structure for 20 ns. MDS showed the importance of the real time dynamic analysis. Relations between the properties of potent antagonists and binding site residues were sought and the possible binding orientations of antagonists were deduced. Comparative analysis of CCR2/CCR5 binding sites was done to facilitate the development of dual antagonists and also to shed lights on the issue of selectivity. The results of the present study may be valuable for further studies on site-directed mutagenesis or structure-based drug design.

## References

- [1] F. Sallusto, M. Baggiolini, Chemokines and leukocyte traffic, *Nat. Immunol.* 9 (2008) 949–952.
- [2] A. Viola, A.D. Luster, Chemokines and their receptors: Drug targets in immunity and inflammation, *Annu. Rev. Pharmacol. Toxicol.* 48 (2008) 171–197.
- [3] L. Yang, C. Zhou, L. Guo, G. Morriello, G. Butora, A. Pasternak, W.H. Parsons, Discovery of 3,5-bis(trifluoromethyl) benzyl L-arylglycinamide based potent CCR2 antagonists, *Bioorg. Med. Chem. Lett.* 16 (2006) 3735–3739.
- [4] G. Butora, G.J Morriello, S. Kothandaraman, D. Guiadeen, A. Pasternak, W. H. Parsons, M. MacCoss, P.P Vicario, M.A Cascieri, L. Yang, S4-Amino-2-alkyl-butiramides as small molecule CCR2 antagonists with favorable pharmacokinetic properties, *Bioorg. Med. Chem. Lett.* 16 (2006) 4715–4722.
- [5] A.B. Pinkerton, D. Huang, R.V. Cube, J.H. Hutchinson, M. Struthers, J.M. Ayala, P.P. Vicario, S.R. Patel, T. Wisniewski, J.A. DeMartinob, J.M. Vernier, Diaryl substituted pyrazoles as potent



CCR2 receptor antagonists, *Bioorg. Med. Chem. Lett.* 17 (2007) 807–813.

- [6] T. Mirzadegan, F. Diehl, B. Ebi, S. Bhakta, I. Polsky, D. McCarley, M. Mulkins, G.S. Weatherhead, J.M. Lapierre, J. Dankwardt, D. Jr. Morgans, R. Wilhelm, K. Jarnagin, Identification of the binding site for a novel class of CCR2b chemokine receptor antagonists: binding to a common chemokine receptor motif within the helical bundle, *J. Biol. Chem.* 275 (2000) 25562–25571.
- [7] C.L. Tsou, W. Peters, Y. Si, S. Slaymaker, A.M. Aslanian, S.P. Weisberg, M. Mack, I.F. Charo, Critical roles for CCR2 and MCP-3 in monocyte mobilization from bone marrow and recruitment to inflammatory sites, *J. Clin. Invest.* 117 (2007) 902–909.
- [8] P.M. Murphy, International Union of Pharmacology. XXX. Update on chemokine receptor nomenclature, *Pharmacol. Rev.* 54 (2002) 227–229.
- [9] C. Gerard, B.J. Rollins, Chemokines and disease, *Nat. Immunol.* 2 (2001) 108–115.

- [10] I.F. Charo, R. M. Ransohoff, The many roles of chemokines and chemokine receptors in inflammation, *N. Engl. J. Med.* 354 (2006) 610–621.
- [11] L. Boring, J. Gosling, S.W. Chensue, S.L. Kunkel, R.V. Jr. Farese, H.E. Broxmeyer, I.F. Charo, Impaired monocyte migration and reduced type 1 (Th1) cytokine responses in C-C chemokine receptor 2 knockout mice, *J. Clin. Invest.* 100 (1997) 2552–2561.
- [12] W.A. Kuziel, S.J. Morgan, T.C. Dawson, S. Griffin, O. Smithies, K. Ley, N. Maeda, Severe reduction in leukocyte adhesion and monocyte extravasation in mice deficient in CC chemokine receptor 2, *Proc. Natl. Acad. Sci. USA.* 94 (1997) 12053–12058.
- [13] T. Kurihara, D. Warr, J. Loy, R. Bravo, Defects in macrophage recruitment and host defense in mice lacking the CCR2 chemokine receptor, *J. Exp. Med.* 186 (1997) 1757–1762.
- [14] B. Lu, B.J. Rutledge, L. Gu, J. Fiorillo, N.W. Lukacs, S.L. Kunkel, R. North, C. Gerard, B.J. Rollins, Abnormalities in monocyte recruitment and cytokine expression in monocyte chemoattractant protein 1-deficient mice, *J. Exp. Med.* 187 (1998) 601– 608.

- [15] M. Mack, J. Cihak, C. Simonis, B. Luckow, A.E. Proudfoot, J. Plachy, H. Bruhl, M. Frink, H.J. Anders, V. Vielhauer, J. Pfirstinger, M. Stangassinger, D. Schlondorff, Expression and characterization of the chemokine receptors CCR2 and CCR5 in mice, *J. Immunol.* 166 (2001) 4697– 4704.
- [16] C.M. Brodmerkel, R. Huber, M. Covington, S. Diamond, L. Hall, R. Collins, L. Leffet, K. Gallagher, P. Feldman, P. Collier, M. Stow, X. Gu, F. Baribaud, N. Shin, B. Thomas, T. Burn, G. Hollis, S. Yeleswaram, K. Solomon, S. Friedman, A. Wang, C.B. Xue, R.C. Newton, P. Scherle, K. Vaddi, Discovery and pharmacological characterization of a novel rodent-active CCR2 antagonist, INCB3344, *J. Immunol.* 175 (2005) 5370 –5378.
- [17] L. Boring, J. Gosling, S.W. Chensue, S.L. Kunkel, R.V. Jr. Farese, H.E. Broxmeyer, I.F. Charo, Impaired monocyte migration and reduced type 1 (Th1) cytokine responses in C-C chemokine receptor 2 knockout mice, *J. Clin. Invest.* 100 (1997) 2552–2561.
- [18] W.A. Kuziel, S.J. Morgan, T.C. Dawson, S. Griffin, O. Smithies, K. Ley, N. Maeda, Severe reduction in leukocyte adhesion and

monocyte extravasation in mice deficient in CC chemokine receptor 2, *Proc. Natl. Acad. Sci. USA.* 94 (1997) 12053–12058.

- [19] T. Kurihara, G. Warr, J. Loy, R. Bravo, Defects in macrophage recruitment and host defense in mice lacking the CCR2 chemokine receptor, *J. Exp. Med.* 186 (1997) 1757–1762.
- [20] B. Lu, B.J. Rutledge, L. Gu, J. Fiorillo, N.W. Lukacs, S.L. Kunkel, R. North, C. Gerard, B.J. Rollins, Abnormalities in monocyte recruitment and cytokine expression in monocyte chemoattractant protein 1-deficient mice, *J. Exp. Med.* 187 (1998) 601– 608.
- [21] N.V. Serbina, T.P. Salazar-Mather, C.A. Biron, W.A. Kuziel, E.G. Pamer, TNF/iNOS-producing dendritic cells mediate innate immune defense against bacterial infection, *Immunity* 19 (2003) 59 –70.
- [22] N.V. Serbina, E.G. Pamer, Monocyte emigration from bone marrow during bacterial infection requires signals mediated by chemokine receptor CCR2, *Nat. Immunol.* 7 (2006) 311–317.
- [23] Y. Huo, C. Weber, S.B. Forlow, M. Sperandio, J. Thatte, M. Mack, S. Jung, D.R. Littman, K. Ley, The chemokine KC, but not monocyte chemoattractant protein-1, triggers monocyte arrest on

early atherosclerotic endothelium, *J. Clin. Invest.* 108 (2001) 1307–1314.

- [24] K. Srikanth, P.C. Nair, M.E. Sobhia, Probing the structural and topological requirements for CCR2 antagonism: Holographic QSAR for indolopiperidine derivatives, *Bioorg. Med. Chem. Lett.* 18 (2008) 1450–1456.
- [25] C. Rolland, R. Gozalbes, E. Nicolai, M.F. Paugam, L. Coussy, F. Barbosa, D. Horvath, F. Revah, G-protein-coupled receptor affinity prediction based on the use of a profiling dataset: QSAR design, synthesis, and experimental validation, *J. Med. Chem.* 48 (2005) 6563–6574.
- [26] T.A. Berkhout, F.E. Blaney, A.M. Bridges, D.G. Cooper, I.T. Forbes, A.D. Gribble, P.H.E. Groot, A. Hardy, R.J. Ife, R. Kaur, K.E. Moores, H. Shillito, J. Willetts, J. Witherington, CCR2: characterization of the antagonist binding site from a combined receptor modeling/mutagenesis approach, *J. Med. Chem.* 46 (2003) 4070–4086.

- [27] T.G. Marshall, R.E. Lee, F.E. Marshall, Common angiotensin receptor blockers may directly modulate the immune system via VDR, PPAR and CCR2b, *Theor. Biol. Med. Model.* 10 (2006) 3.
- [28] W.J. Moree, K. Kataoka, M.M. Ramirez-Weinhouse, T. Shiota, M. Imai, T. Tsutsumi, M. Sudo, N. Endo, Y. Muroga, T. Hada, Potent antagonists of the CCR2b receptor. Part 3: SAR of the (R)-3-aminopyrrolidine series, *Bioorg. Med. Chem. Lett.* 18 (2008) 1869-1873.
- [29] R.J. Cherney, D.J. Nelson, Y.C. Lo, G. Yang, P.A. Scherle, H. Jezak, K.A. Solomon, P.H. Carter, C.P. Decicco, Synthesis and evaluation of cis-3, 4-disubstituted piperidines as potent CC chemokine receptor 2 (CCR2) antagonists, *Bioorg. Med. Chem. Lett.* 18 (2008) 5063-5065.
- [30] G. Kothandan, C.G. Gadhe, T. Madhavan, S.J. Cho, Binding Site Analysis of CCR2 Through In Silico Methodologies: Docking, CoMFA, and CoMSIA, *Chem. Biol. Drug Des.* 78 (2011) 161-174.
- [31] B. Wu, E.Y. Chien, C.D. Mol, G. Fenalti, W. Liu, V. Katritch, R. Abagyan, A. Brooun, P. Wells, F.C. Bi, D.J. Hamel, P. Kuhn, T.M. Handel, V. Cherezov, R.C. Stevens, Structures of the CXCR4

Chemokine GPCR with Small-Molecule and Cyclic Peptide Antagonists, *Science* 330 (2010) 1066-1071.

- [32] S.F. Altschul, W. Gish, W. Miller, E.W. Myers, D.J. Lipman, Basic local alignment search tool, *J. Mol. Biol.* 215 (1990) 403-410.
- [33] S.F. Altschul, T.L. Madden, A.A. Schaffer, J. Zhang, Z. Zhang, W. Miller, D.J. Lipman, Gapped BLAST and PSI-BLAST: a new generation of protein database search programs, *Nucleic. Acids. Res.* 25 (1997) 3389-3402.
- [34] H.M. Berman, J. Westbrook, Z. Feng, G. Gilliland, T.N. Bhat, H. Weissig, I.N. Shindyalov, P.E. Bourne, The protein data bank, *Nucleic. Acids. Res.* 28 (2000) 235-242.
- [35] J.D. Thompson, D.G. Higgins, T.J. Gibson, CLUSTAL W: improving the sensitivity of progressive multiple sequence alignment through sequence weighting, position-specific gap penalties and weight matrix choice, *Nucleic. Acids. Res.* 22 (1994) 4673-4680.
- [36] N. Eswar, B. John, N. Mirkovic, A. Fiser, V.A. Ilyin, U. Pieper, A.C. Stuart, M.A. Marti-Renom, M.S. Madhusudhan, B. Yerkovich, A. Sali, Tools for comparative protein structure modeling and analysis, *Nucleic. Acids. Res.* 31 (2003) 3375-3380.

- [37] A. Sali, T.L. Blundell, Comparative protein modeling by satisfaction of spatial restraints, *J. Mol. Biol.* 234 (1993) 779-815.
- [38] A. Fiser, R.K. Do, A. Sali, Modeling of loops in protein structures, *Protein Sci.* 9 (2002) 1753-1773.
- [39] SYBYL 8.1, Tripos International, 1699 South Hanley Rd., St. Louis, Missouri, 63144, USA.
- [40] R.A. Laskowski, M.W. MacArthur, D.S. Moss, J.M. Thornton, PROCHECK - a program to check the stereochemical quality of protein structures, *J. Appl. Cryst.* 26 (1993) 283-291.
- [41] C. Colovos, T.O. Yeates, Verification of protein structures: patterns of non bonded atomic interactions, *Protein Sci.* 2 (1993) 1511-1519.
- [42] X. Zhang, H. Hufnagel, C. Hou, E. Opas, S. Mckenney, C. Crysler, J. O'neill, D. Johnson, Z. Sui, Design, synthesis and SAR of indazole and benzoisoxazole containing 4-azetidiny-1-aryl-cyclohexanes as CCR2 antagonists, *Bioorg. Med. Chem. Lett.* 21 (2011) 6042-6048.
- [43] M. Clark M, R.D. Cramer, N. Vanopdenbosch, Validation of the general-purpose Tripos 5.2 force-field, *J. Comput. Chem.* 10 (1989) 982-1012.



- [44] M.J.D. Powell, Restart procedures for the conjugate gradient method, *Math Program.* 12 (1977) 241–254.
- [45] J. Gasteiger, M. Marsili, Iterative partial equalization of orbital electronegativity – a rapid access to atomic charges, *Tetrahedron.* 36 (1980) 3219–3228.
- [46] G.M. Morris, D.S. Goodsell, R.S. Halliday, R. Huey, W.E. Hart, R.K. Belew, A.J. Olson, Automated docking using a Lamarckian genetic algorithm and an empirical binding free energy function, *J. Comput. Chem.* 19 (1998) 1639-1662.
- [47] C. Oostenbrink, A. Villa, A.E. Mark, W.F. Van Gunsteren, A biomolecular force field based on the free enthalpy of hydration and solvation: the GROMOS force-field parameter sets 53A5 and 53A6, *J. Comput. Chem.* 25 (2004) 1656-1676.
- [48] D.P. Tieleman, J.L. MacCallum, W.L. Ash, C. Kandt, Z.T. Xu, L. Monticelli, Membrane protein simulations with a united-atom lipid and all-atom protein model: lipid–protein interactions, side chain transfer free energies and model proteins, *J. Phys. Condens. Matter.* 18 (2006) S1221–S1234.

- [49] C. Kandt, W.L. Ash, D.P. Tieleman, Setting up and running molecular dynamics simulations of membrane proteins, *Methods*. 41 (2007) 475-488.
- [50] W.L. Jorgensen, J. Chandrasekhar, J.D. Madura, R.W. Impey, M.L. Klein, Comparison of simple potential functions for simulating liquid water, *J. Chem. Phys.* 79 (1983) 926-935.
- [51] D.M.F. Aalten, R. Bywater, J.B.C. Findlay, M. Hendlich, R.W.W. Hooft, G. Vriend, PRODRG, a program for generating molecular topologies and unique molecular descriptors from coordinates of small molecules, *J. Comput. Aided Mol. Design*, 10 (1996) 255-262.
- [52] J.A. Lemkul, W.J. Allen, D.R. Bevan, Practical Considerations for Building GROMOS-Compatible Small-Molecule Topologies, *J. Chem. Inf. Model*, 50 (2010) 2221-2235.
- [53] T. Darden, D. York, L. Pedersen, Particle mesh ewald—an  $n \cdot \log(n)$  method for ewald sums in large systems, *J. Chem. Phys.* 98 (1993) 10089–10092.
- [54] B. Hess, H. Bekker, H.J.C. Berendsen, J.G.E.M. Fraaije, LINCS: a linear constraint solver for molecular simulations, *J. Comput. Chem.* 18 (1997) 1463-1472.

- [55] S. Miyamoto, P.A. Kollman, Settle, An analytical version of the SHAKE and RATTLE algorithm for rigid water molecules, *J. Comput. Chem.* 13 (1992) 952-962.
- [56] P.J. Carter, A.J. Tebben, The Use of Receptor Homology Modeling to Facilitate the Design of Selective Chemokine Receptor Antagonists, *Methods. Enzymol.* 461 (2009) 249-279.
- [57] C.M. Brodmerkel, R. Huber, M. Covington, S. Diamond, L. Hall, R. Collins, L. Leffet, K. Gallagher, P. Feldman, P. Collier, M. Stow, X. Gu, F. Baribaud, N. Shin, B. Thomas, T. Burn, G. Hollis, S. Yeleswaram, K. Solomon, S. Friedman, A. Wang, C.B. Xue, R.C. Newton, P. Scherle, K. Vaddi, Discovery and pharmacological characterization of a novel rodent-active CCR2 antagonist, INCB3344, *J. Immunol.* 175 (2005) 5370-5378.
- [58] I.F. Charo, W. Peters, Chemokine receptor 2 (CCR2) in atherosclerosis, infectious diseases, and regulation of T-cell polarization, *Microcirculation.* 10 (2003) 259-264.
- [59] K. Srikanth K, P.C. Nair, M. Elizabeth Sobhia, Probing the structural and topological requirements for CCR2 antagonism: holographic

QSAR for indolopiperidine derivatives, *Bioorg. Med. Chem. Lett.* 18 (2008) 1450–1456.

- [60] P.C. Nair, M. Elizabeth Sobhia, Fingerprint directed Scaffold Hopping for identification of CCR2 antagonists, *J. Chem. Inf. Model.* 48 (2008) 1891–1902.
- [61] J.H. Kim, J.W. Lim, S.W. Lee, K. Kim, K.T. No, Ligand supported homology modeling and docking evaluation of CCR2: docked pose selection by consensus scoring, *J. Mol. Model.* 17 (2011) 2707–2716.
- [62] S.R. Kimura, A.J. Tebben, D.R. Langley, Expanding GPCR homology model binding sites via a balloon potential: A molecular dynamics refinement approach, *Proteins* 71 (2008) 1919-1929.
- [63] X.F. Shi, S. Liu, J. Xiangyu, Y. Zhang, J. Huang, S. Liu, C.Q. Liu, Structural analysis of human CCR2b and primate CCR2b by molecular modeling and molecular dynamics simulation, *J. Mol. Model.* 8 (2002) 217-222.
- [64] M.A. Gavrilin, I.V. Gulina, T. Kawano, S. Dragan, L. Chakravarti, P.E. Kolattukudy, Site- directed mutagenesis of CCR2 identified amino acid residues in transmembrane helices 1, 2, and 7 important

for MCP-1 binding and biological functions, *Biochem. Biophys. Res. Commun.* 327 (2005) 533-540.

- [65] G. Kothandan, C.G. Gadhe, S.J. Cho, Structural insights from binding poses of CCR2 and CCR5 with clinically important antagonists: a combined in silico study, *Plos One.* 7 (2012) e32864.
- [66] C.G. Gadhe, S.H. Lee, T. Madhavan, G. Kothandan, D. Choi, S.J. Cho, Ligand Based CoMFA, CoMSIA and HQSAR Analysis of CCR5 Antagonists, *Bull. Korean Chem. Soc.* 31(2010) 2761-2770.

# **Appendix**

## **Appendix A**

### **Acknowledgments**

In the name of God, most Gracious, most Merciful.

I wish to express my sincere appreciation to those who have contributed to this thesis and supported me in one way or the other during this amazing journey. Well, the list of the people I need to thank will not fit to a single Acknowledgement section. I just mention some people whose contribution is obvious.

Completing my PhD degree is probably the most challenging activity of my first 27 years of my life. The best and worst moments of my doctoral journey have been shared with many people. It has been a great privilege to spend some years in the Department of Bio New Drug Development at Chosun University, School of Medicine, and its members will always remain dear to me.

First of all, I am extremely grateful and would like to express my heartfelt gratitude to my lovable advisor, **Professor Seung Joo Cho**, for his guidance and all the useful discussions, especially during the difficult conceptual development stage. His deep insights helped me at various stages of my research. I also remain indebted for his understanding and support during the times when I was really down and depressed. The completion of my doctoral studies would not have been possible without the help of many people.

Special thanks to my thesis committee for their support, guidance and helpful suggestions. Their guidance has served me well and I owe them my heartfelt appreciation.

I would like to thank **Professor Niranjali Devaraj**, **Professor Gunasekaran** and **Dr. Thirumurthy Madhavan** for their wonderful assistance and support to pursue my doctoral degree. Without them, I wouldn't have got the opportunity and courage to pursue my doctoral degree.

I would also like to thank my colleague, lab mate, friend and brother **Mr. Changdev Gadhe** who spent four years of his valuable time with me. We had great scientific discussions, personal sharing's, mutual understanding and care. I also take this opportunity to thank my roommate **Hariharasudhan** for his love and care.

Great thanks to my boundless and lovable friends (N4 guys) in India. They were sources of laughter, joy, and support. I would like to thank my dear friends **Pradeep Kumar**, **Vinoth**, **Jayan**, **Sasi**, **Perumal** and **Napolean** whole heartedly with joy of tears. Words are literally not there to praise their love and affection towards me. Thanks a ton guys.

A special thanks to my ever loving friend **Anand Gowrishankar**. He has been a pillar of strength who taught many a things in my life. A great person by himself helped me to overcome my shyness, immaturity and so and so from my college days. I should thank him for everything he did for me.



The chain of my gratitude would be definitely incomplete if I would forget to thank my master degree friends **Niyaz, Rao, Kalai, Kumaresan, Balaji, Arun**. A special thanks to my master's degree classmate **Shruthi Krishnamurthy**, who has helped me in writing my first research paper. I also like to thank **Dr. Bijoy Swaminathan, Dr. Kathiravan, Inbarasan** and **Sudhan** for sharing a nice relationship with me. I would take this prospect to thank special people named as **Baek jung yoon** and **Sung il**, for helping me personally throughout my stay in Korea. Exceptional thanks to **Professor Jeong Hwan Park** for her love and the opportunity to teach about India and Indian culture to her students. I would also like to thank my school friends, college friends, Madras university friends, Chosun university friends, Indian friends in Korea and all my Korean friends.

Words cannot express the feelings I have for my parents and my brother for their constant unconditional support. I wish to thank my parents, **Mr. A. Kothandan** and **Manimekalai Kothandan**. A special thanks to my dear brother **Madhan** for his support and love. Their love provided my inspiration and was my driving force. I owe them everything and wish I could show them just how much I love and appreciate them.

Finally, I would like to dedicate this work to all. I hope that this work makes you proud.

## Appendix B

### List of Publication

1. Madhavan T., Gadhe C.G., **Kothandan G.**, Cho S.J., Enhancement of P-glycoprotein modulators of arylmethylaniline derivatives: an integrative modeling approach. *Med. Chem. Res.*, 22 (2013) 2511-2523.
2. **Kothandan G.**, Gadhe C.G., Cho S.J., Theoretical characterization of Galanin receptor type 3 (Gal3) and its interaction with agonist (GALANIN) and antagonists (SNAP 37889 and SNAP 398299): An in silico analysis. *Chem. Biol. Drug Des.*, 81 (2013) 757-774.
3. Gadhe C.G., **Kothandan G.**, Cho S.J., Binding site exploration of CCR5 using in silico methodologies: a 3D-QSAR approach. *Arch. Pharm. Res.*, 1 (2013) 6-31.
4. **Kothandan G.**, Madhavan T., Gadhe C.G., Cho S.J., A combined 3D QSAR and pharmacophore-based virtual screening for the identification of potent p38 MAP kinase inhibitors: an in silico approach. *Med. Chem. Res.*, 22 (2013) 1773-1787.
5. Gadhe C.G., **Kothandan G.**, Cho S.J., Computational modeling of human coreceptor CCR5 antagonist as a HIV-1 entry inhibitor: using an integrated homology modeling, docking, and membrane molecular dynamics simulation

- analysis approach. J. Biomol. Struct. Dyn., (2012)  
DOI:10.1080/07391102.2012.732342.
6. Gadhe C.G., **Kothandan G.**, Cho S.J. Large variation in electrostatic contours upon addition of steric parameters and the effect of charge calculation schemes in CoMFA on mutagenicity of MX analogues. Mol. Simulat., 38 (2012) 861-871.
  7. **Kothandan G.**, Gadhe C.G., Cho S.J., Structural insights from binding poses of CCR2 and CCR5 with clinically important antagonists: a combined in silico study. PLoS ONE, 7 (2012) e32864.
  8. Madhavan T., Chung J.Y., **Kothandan G.**, Gadhe C.G., Cho S.J., 3D-QSAR studies of JNK1 inhibitors utilizing various alignment methods. Chem. Biol. Drug Des., (2012) 79 53-67.
  9. **Kothandan G.**, Gadhe C.G., Madhavan T., Choi C.H., Cho S.J., Docking and 3D-QSAR (quantitative structure activity relationship) studies of flavones, the potent inhibitors of p-glycoprotein targeting the nucleotide binding domain. Eur. J. Med. Chem., 46 (2011) 4078-4088.
  10. Gadhe C.G., **Kothandan G.**, Madhavan T., Cho S.J., Molecular modeling study of HIV-1 gp120 attachment inhibitors. Med. Chem. Res., 21 (2011) 1892-1904.

11. Madhavan T., Gadhe C.G., **Kothandan G.**, Lee K., Cho S.J., Various Atomic Charge Calculation Schemes of CoMFA on HIF-1 Inhibitors of Moracin Analogs. *Int. J. Quant. Chem.*, 112 (2011) 995-1005.
12. Madhavan T., **Kothandan G.**, Gadhe C.G., Cho S.J., QSAR analysis on Pfk7 inhibitors using HQSAR, CoMFA, and CoMSIA. *Med. Chem. Res.*, 21 (2011) 681-693.
13. **Kothandan G.**, Gadhe C.G., Madhavan T., Cho S.J., Binding site analysis of CCR2 through in silico methodologies: docking, CoMFA, and CoMSIA. *Chem. Biol. Drug Des.*, 78 (2011) 161-174.
14. Gadhe C.G., Madhavan T., **Kothandan G.**, Cho S.J., In silico quantitative structure-activity relationship studies on P-gp modulators of tetrahydroisoquinoline-ethyl-phenylamine series. *BMC Struct. Biol.*, 11 (2011) 5.
15. Gadhe C.G., Madhavan T., **Kothandan G.**, Lee T.B., Lee K., Cho S.J. Various Partial Charge Schemes on 3D-QSAR Models for P-gp Inhibiting Adamantyl Derivatives. *Bull. Korean Chem. Soc.*, 32 (2011) 1604-1612.
16. Gadhe C.G., Lee S.H., Madhavan T., **Kothandan G.**, Choi D., Cho S.J., Ligand Based CoMFA, CoMSIA and HQSAR Analysis of CCR5 Antagonists. *Bull. Korean Chem. Soc.*, 31 (2010) 2761-2770.

17. Li MH, **Kothandan G**, Cho SJ, Huong PT, Nan YH, Lee KY, Shin SY, Yea SS, Jeon YJ. Magnolol Inhibits LPS-induced NF- B/Rel Activation by Blocking p38 Kinase in Murine Macrophages. *Korean J Physiol Pharmacol.*, 14 (2010) 353-358.